Comparison of POAM III ozone measurements with correlative aircraft and balloon data during SOLVE

Jerry D. Lumpe & Mike Fromm
Computational Physics, Inc., Springfield, VA.

Karl Hoppel & Richard M. Bevilacqua
Naval Research Laboratory, Washington DC.

Cora E. Randall
Laboratory for Atmospheric & Space Physics, University of Colorado, Boulder, CO

Edward V. Browell & William B. Grant
Atmospheric Sciences Research, NASA Langley Research Center, Hampton, VA

Thomas McGee & John Burris
NASA Goddard Space Flight Center, Greenbelt, MD

Laurence Twigg
Science Systems and Applications, Inc, Lanham, MD

Erik C. Richard
Aeronomy Laboratory, National Oceanic and Atmospheric Administration, Boulder, CO

Geoffrey C. Toon, James J. Margitan, & Bhaswar Sen
Jet Propulsion Laboratory, California Institute of Technology, Pasadena, CA

Klaus Pfeilsticker, Hartmut Boesch, & Richard Fitzenberger
Institut fuer Umweltphysik, University Heidelberg, Heidelberg, Germany

Florence Goutail & Jean-Pierre Pommereau
Service d'Aeronomie du CNRS
BP3, 91371 VERRIERES LE BUISSON, France

Abstract

The Polar Ozone and Aerosol Measurement (POAM) III instrument operated continuously during the SOLVE mission, making approximately 1400 ozone profile measurements at high-latitudes both inside and outside the Arctic polar vortex. The wealth of ozone measurements obtained from a variety of instruments and platforms during SOLVE provided a unique opportunity to compare correlative measurements with the POAM III dataset. In this paper we validate the POAM III version 3.0 ozone against measurements from seven different instruments that operated as part of the combined SOLVE/THESEO 2000 campaign. These include the airborne UV Differential Absorption Lidar (UV DIAL) and the Airborne Raman Ozone and Temperature Lidar (AROTEL) instruments on the DC-8, the dual-beam UV-Absorption Ozone Photometer on the ER-2, the MkIV Interferometer balloon instrument, the Laboratoire de Physique Molèculaire et Applications and Differential Optical Absorption Spectroscopy (LPMA/DOAS) balloon gondola, the JPL *in situ* Ozone instrument on the OMS balloon platform, and the Système D'Analyse par Observations Zénithales (SAOZ) balloon sonde. The resulting comparisons show a remarkable degree of consistency despite the very different measurement techniques inherent in the datasets, and thus provide a strong validation of the POAM III version 3.0 ozone. This is particularly true in the primary 14 to 30 km region, where there are significant overlaps with all seven instruments. At these altitudes POAM III agrees with all the datasets to within 7-10 % with no detectable bias. The observed differences are within the combined errors of POAM III and the correlative measurements. Above 30 km, only a handful of SOLVE correlative measurements exist and the comparisons are highly variable, and therefore the results are inconclusive. Below 14 km the SOLVE comparisons also show a large amount of scatter and it is

difficult to evaluate their consistency, although the number of correlative measurements is large. The UV DIAL, DOAS, and JPL/OMS comparisons show differences of up to 15 % but no consistent bias. The ER-2, MkIV and SAOZ comparisons, on the other hand, indicate a high POAM bias of 10 - 20 % at the lower altitudes. In general the SOLVE validation results presented here are consistent with the validation of the POAM III version 3.0 ozone using Stratospheric Aerosol and Gas Experiment (SAGE) II and Halogen Occultation Experiment (HALOE) satellite data, and *in situ* ECC ozonesonde data.

1. Introduction

The objectives of the SAGE III Ozone Loss and Validation Experiment (SOLVE) campaign were to examine the processes controlling ozone at mid- to high-latitudes and to acquire multiple correlative data sets for validation of the Stratospheric Aerosol and Gas Experiment (SAGE) III instrument. Successful completion of this objective required a coordinated campaign of measurements in the Arctic high-latitude region using a variety of instruments and platforms. These included the NASA DC-8 and ER-2 aircraft, as well as balloon platforms, ground-based instruments and satellites. Of the latter the Polar Ozone and Aerosol Measurement (POAM) III instrument was the only source of high-latitude satellite vertical profile measurements used in the SOLVE campaign.

The initial motivation for introducing POAM III as a component of SOLVE was primarily because its latitude coverage and measurement suite make it an ideal validation platform for SAGE III. Figure 1 shows the POAM III latitude coverage in the Northern Hemisphere compared to the predicted SAGE III ephemeris. The two instruments' coverage overlaps a number of times during the year, providing multiple opportunities for comparison. Furthermore POAM III measures the same primary species as SAGE III – ozone, water vapor, nitrogen dioxide and aerosol extinction. Both POAM III and its predecessor POAM II have used SAGE II extensively in their satellite validation studies [*Rusch et al*., 1997, 2001; *Randall et al*., 2000, 2001a] and it is expected that both POAM III and SAGE III will eventually benefit from a detailed retrieval comparison.

Of course, due to unforeseen launch delays, the SAGE III instrument was not operational during the SOLVE campaign. Nevertheless, the wealth of high-latitude measurements made during SOLVE provide a valuable resource for validation of the POAM III dataset. In this paper we present validation of the POAM III version 3.0 ozone using a number of coincident ozone measurements obtained during SOLVE. This study complements POAM III ozone validation efforts which concentrate on comparisons with other satellite data sets and ECC ozonesondes [*Rusch et al*., 2001]. The POAM III/SOLVE ozone validation presented here includes aircraft and balloon data (both *in situ* and remotely sensed).

This paper is not intended as a comprehensive intercomparison of the various SOLVE ozone data sets but is presented strictly from the point of view of POAM III validation. In addition to further quantifying the quality and scientific validity of the POAM III ozone data, it is hoped that this study will prove useful in planning future validation efforts for SAGE III. Absent an actual POAM III/SAGE III validation study, which will have to await the SAGE III launch in 2001, we feel this is one of the most useful contributions to SAGE III resulting from the POAM III involvement in SOLVE. Of course, by helping to validate the POAM III data products, this effort will directly benefit the SAGE III validation in the future.

In this work, the POAM III ozone measurements are compared with measurements from seven different instruments that operated as part of the combined SOLVE/THESEO 2000 campaign. These include the airborne UV Differential Absorption Lidar (UV DIAL) and the Airborne Raman Ozone and Temperature Lidar (AROTEL) instruments on the DC-8, the dual-beam UV-Absorption Ozone Photometer on the ER-2, the MkIV balloon interferometer, the Laboratoire de Physique Molèculaire et Applications and Differential Optical Absorption Spectroscopy (LPMA/DOAS) balloon gondola, the JPL *in situ* Ozone instrument on the Observations of the Middle

Stratosphere (OMS) balloon platform, and the Système D'Analyse par Observations Zénithales (SAOZ) balloon sonde. We first quantify the agreement between POAM III and each of these instruments separately and then compare the results to see if they give a consistent picture of the POAM III ozone validation, as well as maintaining consistency with the satellite and ECC ozonesonde validation studies. We begin with an overview of the POAM III ozone measurements and current status of the version 3.0 validation in Section 2. In section 3 we compare the DC-8 data sets (UV DIAL and AROTEL), followed by the ER-2 comparisons in section 4, MkIV in section 5, DOAS in section 6, OMS/JPL Ozone in section 7, and finally the SAOZ comparisons in section 8. Section 9 contains a summary and conclusions.

2. Overview of POAM III measurements and version 3.0 ozone validation

The POAM III instrument is a nine-channel photometer that employs the technique of solar occultation to derive composition and temperature throughout the stratosphere and upper troposphere. By measuring atmospheric extinction in select bands from 0.354 to 1.018 μm it is possible to retrieve density profiles of ozone, nitrogen dioxide and water vapor, as well as temperature and wavelength-dependent aerosol extinction. The instrument and its basic operational characteristics are described in detail in *Lucke et al.* [1999].

POAM III has been in routine operation on the SPOT 4 satellite since April 24, 1998. It makes 14 measurements per day in each hemisphere, at approximately constant latitude but separated in longitude by 25 degrees. This relatively coarse horizontal sampling pattern is a consequence of the solar occultation geometry. Northern Hemisphere (NH) measurements are made at satellite sunrise but actually correspond to local sunset due to the retrograde orbit of the satellite. During the SOLVE time period (November 1999 to March 2000) approximately 1400 NH measurements were made at latitudes between 63.5 and 69°N.

Ozone is retrieved operationally between 60 km and a lower limit which is typically in the mid- to upper-troposphere, depending on local cloud top height and atmospheric opacity, which determines the minimum altitude to which the Sun sensor can actively track the Sun. The POAM III version 3.0 retrieval algorithms and error analysis are described in *Lumpe et al*. [2001]. The primary ozone information in the measurements comes from the 603-nm channel, at the peak of the O_3 Chappuis bands. Based on the analysis presented in *Lumpe et al*. [2001] the total random error (precision) of the POAM III ozone retrievals is estimated to be 3-5 % between 12 and 60 km, increasing to 15 % or more at and below 10 km. In the lowermost stratosphere and upper troposphere the ozone retrieval becomes very sensitive to accurate removal of the aerosol extinction component. Maximum systematic errors due to cross section uncertainties are estimated to be at the 1 to 2 % level.

The vertical resolution of the ozone retrieval, as defined by the width of the retrieval averaging kernels, is 1 km throughout the stratosphere but degrades rather quickly to 2-3 km in the upper troposphere [*Lumpe et al*. 2001]. Horizontal resolution perpendicular to the instrument line of sight (i.e., parallel to the terminator) is limited by the size of the solar disk, which is approximately 30 km at the tangent point. Parallel to the line of sight one measure of horizontal resolution can be taken to be the path length of the 1-km vertical shell sampling, which is approximately 200 km. However, this number tends to underestimate the effective horizontal resolution since the information content in the slant path measurement is sharply peaked at the tangent point.

This paper focuses on validation of the POAM III version 3.0 ozone using correlative data obtained during the SOLVE/THESEO 2000 campaign. Preliminary validation of an earlier version of POAM III ozone was presented in *Lucke et al*. [1999]. The version 3.0 ozone has also been validated against version 6.0 Stratosphere Aerosol and Gas Experiment (SAGE) II and version 19 Halogen Occultation Experiment (HALOE) satellite data, and balloon-borne ECC ozonesondes in *Rusch et al*. [2001]. The results of this analysis show that the POAM III NH ozone agrees with SAGE II, HALOE and ECC ozonesondes to within 5 to 7 %, with no bias, in the altitude range from 12 to 50 km. Between 50 and 60 km POAM tends to be biased high with respect to HALOE by 5 – 10 %, but this bias is not seen in the POAM/SAGE II comparisons. Somewhat larger disagreements (15 – 20 %) are seen below 12 km, with POAM III generally biased high relative to both satellites and ECC ozonesondes. Unless otherwise noted, for the remainder of this paper we will refer to POAM III simply as POAM to simplify the notation.

3. DC-8 comparisons.

3.1 Overview of DC-8 coincidences

The flight plans for the DC-8 were constructed specifically to provide a number of direct coincidences with the POAM measurements. These overlaps provide an excellent opportunity to compare measurements made by POAM and the DC-8 instruments in air masses that coincide closely in both time and space. There were six such coincidences during SOLVE, occurring on December 2 & 14, January 16 & 25, and March 3 & 9. On a number of these flights the DC-8 executed multiple passes through the POAM tangent point, in addition to dives, to maximize the number of coincident measurements made by both *in situ* and remote sensing instruments aboard the aircraft.

Figure 2 shows the location of the coincident measurements on each of these six days. The red symbol represents the POAM 20-km tangent point and the red box surrounding this point represents the area defined by the coincidence criteria used in the comparisons. We define a coincidence as any measurements made within ± 1 deg in latitude, ± 2 deg in longitude and ± 1 hour in time. These are significantly tighter criteria than typically used in POAM satellite validation studies, but given the extent of the overlaps they still yield a significant number of coincident measurements, as discussed below. The blue line in Figure 2 represents the DC-8 flight track on each day. Although difficult to see on the scale of this plot the flight path does pass through the coincidence region on all days (more extensively on some days than others). Only those DC-8 measurements made within this red box (and satisfying the time constraint described above) are used in the comparisons. For reference, contours corresponding to the location of the outer, middle and inner edge of the polar vortex at 450 K have also been plotted in the black solid and dashed lines. In Figure 2, and subsequently in this paper, the convention of *Nash et al.* [1996] has been used to define the vortex edge.

These maps are helpful because it is important to take into account the position of the measurements relative to the polar vortex in evaluating the ozone profile comparisons below. For example, Figure 2 shows that on all six days except 12/2/99 the DC-8 traversed at least the inner edge of the vortex sometime during its flight. On three days (12/2/99, 12/14/99 and 3/3/00) the POAM and DC-8 coincidences occur well inside the vortex inner edge whereas on the other days the coincidences are near the vortex edge, where one might expect strong horizontal gradients in the ozone. This will be discussed in more detail below.

In this paper the POAM ozone measurements are compared with the two ozone lidars operating on the DC-8; the NASA Langley UV Differential Absorption Lidar (UV DIAL) and the NASA Goddard Airborne Raman Ozone and Temperature Lidar (AROTEL). Both of these instruments measure the ozone profile above the aircraft and therefore provide significant overlap with the POAM measurements in the low- to mid-stratosphere. There is an added advantage in being able to compare simultaneously with two instruments that are essentially measuring the same air mass continuously. This is a unique opportunity, which is further enhanced by the fact that all three instruments make the same fundamental measurement – ozone concentration as a function of altitude.

3.2 Coincident data sets

The NASA Langley airborne UV Differential Absorption Lidar (UV DIAL) system has been used to measure ozone, aerosol, and cloud profiles during four previous stratospheric ozone investigations, affording the opportunity for many intercomparisons with other ozone measuring instruments [*Browell*, 1989; *Browell et al*., 1990, 1993, 1998; *Grant et al*., 1998]. This system uses two frequency-doubled Nd:YAG lasers to pump two high-conversion-efficiency, frequency-doubled, tunable dye lasers. In stratospheric O_3 investigations, the two frequency-doubled dye lasers are operated independently with one tuned to 301 nm for the O_3 DIAL on-line wavelength and the other tuned to 311 nm for the off-line wavelength. All of the beams are transmitted in the zenith direction through a 40-cm-diameter fused silica window. The atmospheric backscattered laser returns are collected by a 36-cm diameter telescope, optically separated, and directed on to different detectors.

The UV DIAL instrument measures ozone up to 10-15 km above the aircraft with an accuracy of better than 10 %. Vertical resolution of the measurements is 750 m and horizontal resolution is 70 km (5 min). Note that the horizontal and vertical resolutions of the UV DIAL ozone measurements, although slightly better than POAM, are very similar. The UV DIAL ozone has been compared with ECC ozonesonde data from Ny Aalesund (79^o N, 12^o E) during SOLVE [*Grant et al*., manuscript in preparation]. In the 15 – 20 km range the mean difference between the two measurements is ~ 3 % with a standard deviation of 4 %. The sign of the difference is such that UV DIAL tends to biased low relative to the ECC ozonesondes in this altitude range.

The Airborne Raman Ozone, Aerosol and Temperature Lidar (AROTEL) is a DC-8 instrument conceived, designed and built by Goddard Space Flight Center in collaboration with scientists from Langley Research Center. The instrument was flown for the first time during the SOLVE campaign. The instrument is a multi-wavelength lidar: radiation at 1064, 532 and 355 nm are transmitted from a Nd-YAG laser, and 308-nm radiation is transmitted from a XeCl excimer laser. These wavelengths are transmitted nearly simultaneously, and backscattered radiation is collected with a 16" telescope. This returned light at the transmitted wavelengths, as well as Raman scattered radiation at 387 and 332 nm (N_2 scattering from the transmitted 355 and 308 nm beams) is wavelength-separated using dichroic beamsplitters and detected using Hamamatsu R7400P phototubes.

Ozone data is extracted from the four UV signals using the differential absorption lidar technique. The algorithm for ozone retrieval is essentially identical to the description in *McGee et al. [1*995], which describes the NDSC ground-based system. The only difference is in the use of a fourth order polynomial fitting function as opposed to the linear function previously described. In order to ensure linearity of signals, multiple detectors are used for each wavelength. Beyond about 3 km above the aircraft the UV signals are all photon counted; analog detection is used near to the aircraft. Vertical resolution of the retrieved ozone profiles is approximately 1 km and the accuracy is better than 10 %. A detailed description of the instrument is given in *McGee et al*. [2001].

3.3 Comparison of POAM, UV DIAL and AROTEL ozone

In this section we first discuss the comparisons between POAM and the two DC-8 instruments individually, and then look at how well the three data sets compare collectively. For simplicity we have plotted the coincident ozone profiles from all three instruments together in Figure 3. In each panel, corresponding to one DC-8 flight date, the black curve represents the single ozone profile measured by POAM at the coincidence location indicated by the red symbol in Figure 2. For the DC-8 instruments, rather than plot all the individual profiles satisfying the coincidence criteria, we have plotted a mean profile for each flight. For the UV DIAL data, plotted in red, this is produced by binning all the coincident data (obtained directly from the SOLVE data archive) in 0.25 km bins and then calculating an average ozone density in each bin. The AROTEL raw data meeting the coincidence criteria were averaged prior to the retrieval of ozone, instead of calculating the average of profiles within the archived data set. This approach permitted the retrieval to reach to higher altitudes than the ozone profile averaging method. The average AROTEL profiles are plotted in blue in Figure 3.

Note that the UV DIAL and AROTEL measurements tend to sample somewhat different vertical regions of the stratosphere. Profiles from the two instruments generally overlap in the altitude range from ~ 14 to 23 km. For the six days of interest in this study ozone retrievals are typically available between about 11 to 23 km for UV DIAL and 14 to 30 km for AROTEL. Exceptions for AROTEL include January 25, where the data below 19 have been removed due to possible PSC contamination and the December 14 and March 9 profiles, which extend all the way to 40 km, but with sharply increasing random error above 30 km (not shown).

In general the POAM and UV DIAL ozone density profiles agree very well. On most flights the vertical structure of the profiles measured by the two instruments are very consistent and the magnitude generally agrees well. Notable exceptions are the low altitude discrepancies on 1/16/00 and 3/3/00 and the fairly bad overall agreement on 3/9/00. The only systematic differences apparent in these comparisons is that POAM tends to be high relative to UV DIAL above about 19 km. It is likely that this is due to the tendency for the UV DIAL measurements to be slightly underestimated at the higher altitudes in sunlit conditions. This tendency has been seen previously in comparisons between UV DIAL and correlative SAGE II and HALOE measurements [*Grant et al.*, 1998].

The low altitude discrepancies on 1/16/00 and 3/3/00 are likely due to mid-latitude intrusions and large gradients in the ozone distribution below 13-14 km, which are readily seen in the UV DIAL flight images on those days. On 3/9/00, where we see the greatest differences in the 14-20 km range, the measurements were very near the vortex edge, and again very large horizontal gradients in ozone are evident in the UV DIAL ozone cross section. Also, on this particular day the DC-8 coincidences were actually biased towards low latitudes relative to the POAM point, which accentuates the sampling bias due to the strong ozone gradients. For these reasons we believe the discrepancies seen on this day, and at the low altitudes on 1/16/00 and 3/3/00, are more indicative of true atmospheric variability than any fundamental error in either measurement.

For the most part Figure 3 also shows quite good agreement between the POAM and AROTEL profiles. Both instruments consistently reproduce small-scale vertical structure in the ozone profile, although the lidar measurements often show more detailed vertical structure than the POAM profiles (see, e.g., the January 16 and 25 profiles). There also appears to be a tendency on some days for POAM to be low relative to AROTEL at the peak of the ozone profile. For the most part however, the agreement in the profiles above 20 km is good, and even up to 40 km for the two AROTEL profiles that extend to that altitude. One notable exception is on March 3, where the AROTEL ozone appears to have a noticeably smaller scale height than POAM above the profile peak. The March 9 POAM/AROTEL comparison, like the POAM/UV DIAL comparison on that day, shows poor agreement overall below 25 km. It is interesting to note, however, that the two lidar profiles themselves do not agree very well on this day, showing very different vertical structure and a clear systematic bias. At the present time this is not understood.

Figure 4 summarizes the ozone differences between POAM and the DC-8 instruments. For each flight the average UV DIAL and AROTEL ozone profiles plotted in Figure 3 were first linearly interpolated to the standard POAM 1-km altitude grid. The relative difference profile (in percent) was then calculated according to

$$\Delta = 200 \times \frac{POAM - Corr}{POAM + Corr} \tag{1}$$

where $Corr$ represents a correlative measurement, in this case UV DIAL or AROTEL. The POAM/UV DIAL and POAM/AROTEL differences are plotted in the top and middle panels, respectively, of Figure 4. In each panel the colored curves (red for UV DIAL, blue for AROTEL) correspond to the individual difference profiles for each flight and the black profile is the mean of all six flights. Error bars correspond to the standard error of the mean difference.

The POAM/UV DIAL mean difference is within 5 to 7 % between 14 and 20 km, and less than 10 % between 13 and 21 km. At the lowest altitude point, 12 km, the mean error is clearly dominated by the large differences on 1/16/00 and 3/3/00 discussed above. Also, the general tendency for UV DIAL to be biased somewhat low relative to POAM above 20 km is evident in the mean. The fact that the UV DIAL ozone is biased low on average by a few percent from 11 to 20 km is consistent with the UV DIAL/ECC comparisons [*Grant et al.*, manuscript in preparation], and probably indicates a slight overestimate in the ozone absorption coefficient used in the DIAL analysis (note, however, this should not affect the trend determination from UV DIAL data). Except for these small systematics, which we feel are understood, the two instruments agree to within the combined measurement uncertainties and these results are generally consistent with previous POAM validation [*Rusch et al.*, 2001].

The mean POAM/AROTEL difference is within 10 % at all altitudes below 37 km. The exception is the localized peak at 28-29 km where differences reach 10 - 20 %, with POAM high (note, however, that this feature is dominated by the December 12 event where the AROTEL profile shows a pronounced minimum at this altitude which is not seen by POAM). The results show a fairly consistent vertical structure in the difference profiles for all days, with differences generally changing from -10 % at 18 km to +10 % at 28 km. Note that above 30 km only two measurements, from the December 14 and March 9 flights, contribute to the mean. While these also appear to be fairly consistent, given the small number of measurements in this altitude range it is difficult to tell how significant this result is. The POAM/AROTEL differences in the 15 to 27 km range are generally consistent with the POAM satellite and ECC ozonesonde validation, although the peak difference of -10 % at 18-19 km (again a fairly systematic feature in the six flights) is larger than the maximum differences seen in *Rusch et al.* [2001].

In summary, the bottom panel of Figure 4 shows the mean difference profiles for the POAM/UV DIAL and POAM/AROTEL comparisons on the same plot. Again, ignoring the POAM/UV DIAL differences above 20 km, POAM agrees with both instruments to within 10 % between 13 and 27 km with larger errors (but oscillating about zero) in the POAM/AROTEL comparisons at the higher altitudes. It is interesting to note that there is a very similar systematic shape to the two mean difference profiles, as well as a nearly constant offset. At this point these correlations in the differences between the UV DIAL and AROTEL comparisons are not understood, but should be explored more in the future.

4. ER-2 comparisons

During the two SOLVE deployments the ER-2 aircraft made a total of 11 science flights out of Kiruna (neglecting transit flights). On each of those flights *in situ* measurements of the ozone concentration were made from the Q-Bay of the aircraft by the dual-beam UV-Absorption Ozone Photometer (hereafter referred to as simply "NOAA Ozone") [*Proffitt et al*., 1989]. The instrument consists of a 254-nm mercury lamp, two sample chambers that can be periodically scrubbed of ozone, and two detectors that measure the radiation directed from the lamp through the chambers. Ozone absorbs strongly at this wavelength and the absorption cross-section is accurately known; hence, the ozone number density can be accurately calculated from the difference in the detected signals from the two chambers. Since the two absorption chambers are identical, virtually continuous measurements of ozone are made by alternating the ambient air sample and ozone scrubbed sample between the two chambers. At a one-second data collection rate, the minimum detectable concentration of ozone (one standard deviation) is 1.5×10^{10} molecules/cm^3 (0.6 ppbv at STP or 8 ppbv at 20 km). Measurement accuracy is predicted to be 3% plus precision [*Proffitt et al*., 1989].

Because the NOAA Ozone measurements are made *in situ* and the aircraft tends to maintain a more or less constant cruise altitude at approximately 18-20 km (aside from takeoff, landing and occasional dives), the POAM/ER-2 comparisons are necessarily heavily weighted to this narrow altitude range. In this region *Rusch et al*. [2001] has shown that the POAM version 3.0 ozone agrees to within 3 - 5 % with coincident satellite and ECC ozonesonde data in the Northern Hemisphere (with POAM in general somewhat low compared to the satellites but high relative to the sondes).

Because of the problematic nature of comparing satellite to *in situ* measurements, we have used three different approaches in comparing the POAM and ER-2 ozone data: vortex-average, trajectory hunting, and direct coincidence measurements. In the first approach, vortex-averaged ozone measurements from each instrument are compared for all of the ER-2 flights. This approach was initially motivated by the observation that the ER-2 ozone data from most of the deep vortex-survey flights generally shows a very uniform ozone field within the interior of the vortex, at least in the early winter (see discussion below). This uniformity is also apparent from the in-vortex measurements made by POAM over time periods of several days. The second method used to compare POAM and ER-2 ozone data involves using a trajectory analysis to identify and directly compare identical air parcels that were sampled by both instruments. Finally, we have also identified and compared standard temporal and spatial coincidences between the POAM and ER-2 ozone measurements. Unlike the DC-8, no effort was made to incorporate specific underflights of the POAM measurement locations into the ER-2 flight plans during SOLVE. However, direct coincidences do exist on a number of days if the coincidence criteria are relaxed considerably from those used for the DC-8 comparisons.

Results from these three different comparison techniques are discussed separately in sections 4.1- 4.3 below. All three techniques have their strengths and shortcomings. The vortex-average method minimizes the effect of random errors, but depends upon having unbiased (or at least the same) ER-2 and POAM vortex sampling. The trajectory hunting method would, in principle, be the best way to ensure comparison of similar air parcels, but it relies on the accuracy of the trajectory analysis. Finally, the direct coincidence technique is the most straightforward and frequently used validation method, but given the well-known trade-offs between constraining the closeness of the coincidences and obtaining a statistically significant number of samples, there is no guarantee that similar air parcels are sampled.

4.1 Vortex-average ozone comparisons

In order to compare the vortex-average ozone measured by POAM and the ER-2 it was first necessary to isolate the in-vortex data obtained by each instrument on a given day. For the ER-2 the N_2O and CO_2 tracer data were used to determine which time segments of the flight corresponded to air sampled well within the interior of the vortex. All data meeting the vortex-discrimination criteria was then binned in uniform 10 K potential temperature bins to create a single vortex-average vertical profile.

As discussed in a companion paper in this special issue [*Randall et al.,* 2001b], POAM routinely made measurements both inside and outside the polar vortex on a daily basis during SOLVE. This is because the center of the vortex was frequently displaced from the pole towards Europe or Asia and therefore POAM, measuring around a circle of latitude, would sample both in-vortex and extra-vortex air on a given day. However, because of the relatively coarse horizontal sampling afforded by the solar occultation technique, on any given day only a handful of events might be well inside the vortex. Therefore, to obtain a statistically meaningful sample of in-vortex ozone measurements for each ER-2 flight day the POAM data were averaged over a three-day time period centered on the flight date (i.e., flight day $\pm$ 1 day). All POAM profiles measured within the inner vortex boundary (as defined by the Nash criteria) in that three-day period were averaged together and interpolated onto the same potential temperature grid as the ER-2 data.

Figure 5 illustrates this procedure for four representative ER-2 flight days. For each day the ER-2 flight track is represented by the solid blue line, the inner and middle Nash vortex edges (at 450 K) are represented by the black and green contours, respectively, and all POAM measurements made during the three-day averaging period are shown as red dots. Only those POAM points and that portion of the ER-2 flight lying within the solid black contour contribute to the vortex-average profile (the POAM vortex discrimination uses the appropriate vortex boundary for each of the three days used in the average). The number of such points of course varies from flight to flight. On ER-2 vortex survey flights, such as 3/5/00, the entire ER-2 flight occurs deep in the vortex whereas other flights contain planned vortex edge crossings.

Figure 6 shows the vortex-average ozone profiles measured by both instruments for the eleven ER-2 science flights out of Kiruna. The red circles represent the POAM points, black squares are the ER-2 points and the solid lines represent $\pm$ one standard deviation of the mean for each flight. Clearly there is generally very good quantitative agreement between the two data sets. POAM does appear biased somewhat low relative to ER-2 on the January 27 and 31 flights, but by no more than 5 %. Figure 6 also shows an increasing tendency for POAM ozone to be high relative to the ER-2 at the higher altitudes in late winter, beginning with the March 5 flight. In this late-winter period the vortex had experienced a large amount of chemical ozone loss [*Hoppel et al*., 2001], and POAM measured large in-vortex ozone gradients [*Randall et al.,* 2001b]. Figure 6 also suggests that while the POAM vortex-average standard deviation is increasing over this late winter period, the ER-2 variation is not. This suggests that the ER-2 was preferentially sampling the most depleted vortex air, while POAM obtained more of a vortex survey. This view is reinforced by Figure 5, which shows the small slice of the vortex sampled by the ER-2 on March 11 relative to the more extensive POAM vortex sampling (the corresponding March 12 map, which is not shown, yields the same conclusion). Of course, it was not atypical for POAM to sample a larger portion of the vortex than the ER-2 throughout the winter. However, increasing ozone gradients within the vortex (as a result of ozone loss) later in the winter would serve to accentuate the effects of this sampling bias. Thus, we suggest that the increasing tendency for POAM to be biased high compared to the ER-2 in the late winter comparisons is much more likely to be the result of sampling biases rather than real measurement differences.

To illustrate this point, in Figure 7 we have plotted the POAM and ER-2 ozone measurements at 460 K as a function of equivalent latitude on January 23 and March 11 (equivalent latitude is the latitude enclosing the same area as a given potential vorticity contour). The red symbols represent all the POAM measurements at 460 K within $\pm$ 1 day of flight date (both inside and outside the vortex) whereas black symbols represent the ER-2 ozone data (in-vortex only). The vertical lines denote the middle and inner vortex edges. On January 23 the ozone inside the vortex, as measured by both instruments, is quite uniform. This situation is typical of the early- and mid-winter flights and, as discussed previously, provided the original justification for using vortex-average comparisons. Clearly the situation is very different by March 11. Here the POAM data show evidence of large ozone gradients within the vortex, with two distinct populations of low and high ozone; the ER-2, however, preferentially samples only that part of the vortex with depleted ozone. This explains why the vortex-averaged POAM ozone on this day, and on all other days in the late winter period, is biased high relative to the ER-2. This is purely a sampling bias, rather than a measurement error.

Finally, we note that the sharp structures in the 1/14/00 and 1/23/00 ER-2 profiles are due to intrusions (mid-latitude filaments) encountered by the ER-2 on those flights. This can be clearly seen by correlating the O_3 and tracer data from different ER-2 instruments on those flights (not shown). While POAM can in principle also see such filaments, there is no guarantee that it sampled these specific features on those days. Even if a filament were seen in one POAM measurement on the flight date it would be smoothed out in the three-day averaging.

In Figure 8 these results are summarized by plotting the average ozone mixing ratio profiles, and their mean difference, for the eleven flights. The mean difference is within 5 % at all levels between 350 and 450 K and within 7 % at 460 K. The only difference greater than 10 % is at the highest theta level, 470 K, which is clearly dominated by sampling biases discussed above. On the whole, the vortex-averaged comparisons show excellent agreement between POAM and ER-2 ozone.

4.2 Trajectory hunting analysis

The second method of comparing POAM and ER-2 measurements is to look for air parcel trajectory matches. Forward and backward isentropic trajectories were run from each POAM measurement location at 10 K increments in the vertical using the UKMO wind analysis. We then searched for cases where these trajectories crossed the ER-2 flight track within the following constraints: 300 km horizontal separation, 5 K separation in the vertical, and 1.2 hours in time. The matches were further constrained to have a maximum trajectory length of $\pm$ 5 days. Of course, it is possible that within five days significant ozone chemical change could occur along the trajectory, but most of the matches found in the analysis were within three days, and fairly evenly distributed between forward and backward trajectories. A total of 249 matches were found to meet the above criteria in the vertical range from 380 to 470 K.

The results of the trajectory hunting analysis are summarized in Figure 9. The small black dots represent the ozone difference for all of the 249 points that satisfied the match criteria. Note that there tends to be more scatter in trajectory-match comparisons relative to the vortex-average comparisons. This is expected both because there is some scatter introduced by trajectory inaccuracies and of course the vortex-average approach, which averages over many measurements, naturally tends to produce a smoother result. The black curve in Figure 9 represents the mean difference for all the match events (after binning the data in 10 K potential temperature bins) and the error bars correspond to the standard error of the mean difference. Comparing this result with Figure 8 shows that the trajectory matching and vortex-average comparisons yield remarkably similar results in terms of both the magnitude and vertical structure of the ozone difference. In particular, it is interesting to note that the high POAM bias above 450 K appears in both analyses. However, close inspection of the trajectory matching results shows that there is no trend toward increasing POAM biases later in the winter as was observed in the vortex-average comparisons. Furthermore, there is no observed bias with respect to forward or backward trajectories, which could produce a bias in the relative differences if chemical depletion is occurring along the trajectories. Therefore, the consistency of this high bias in the two approaches is not currently understood and deserves further study.

4.3 Comparison of POAM/ER-2 direct coincidences

Finally, we present comparisons of POAM measurements made in direct temporal and spatial coincidence with the ER-2 measurements. If the stringent coincidence criteria used in the DC-8 analysis in section 3 are used for the ER-2, very few coincident measurements are found. However, if the criteria are relaxed considerably many more coincident data points are found. For the comparisons presented here we chose the following criteria: ± 3 deg in latitude, ± 10 deg in longitude and ± 3 hour in time. These criteria are similar to those typically used in the POAM satellite validation studies [*Randall et al.*, 2000, 2001a; *Rusch et al.*, 1997, 2001]. We further required that both POAM and ER-2 measurements be made within the inner edge of the vortex.

Coincident POAM and ER-2 measurements satisfying these criteria were found for all the ER-2 flights discussed in section 4.1 except the flight on January 14. In addition, all of these coincident ER-2 measurements contain some portion of the data obtained during takeoff, landing or the executed dives and stack maneuvers. Therefore they all contain ER-2 data over a range of altitudes, which allows for direct profile comparisons with POAM. For these comparisons we plot the coincident POAM and ER-2 data versus altitude since this is the fundamental vertical grid for the POAM data and is also available directly for the ER-2 from the archived GPS altitudes.

Figure 10 shows the coincident POAM (in blue) and ER-2 (in red) ozone mixing ratio profiles for each flight. The ER-2 profiles were constructed by binning all points satisfying the coincidence criteria into 1-km altitude bins and calculating a mean ozone mixing ratio in each bin. The resulting profile was then linearly interpolated to the standard POAM altitude grid. The altitude range of the coincident ER-2 profiles varies considerably from flight to flight but most flights provide a significant overlap with the POAM profiles. In general the agreement is qualitatively quite good, although occasional systematic differences do appear (e.g., January 23 below 16 km, February 2, and March 5). Note that the comparisons do not show the increasing tendency toward higher POAM biases as was seen in the vortex-average and trajectory hunting comparisons. However, there is little direct POAM/ER-2 overlap in the 460-470 K (~ 18 km) region where these biases occur, particularly late in the winter.

Figure 11 shows the mean ozone difference profile (black curve) obtained from averaging the coincident data from all ten flights. The numbers on the right axis represent the number of profiles that contribute to the mean at each altitude level. Between 11 and 19 km the differences are within 10 %. However there is a small but statistically significant bias over most of this altitude range, with POAM higher than ER-2 by an average of ~ 5 %. Below 11 km POAM is systematically higher than ER-2 by approximately 20 % on average.

For comparison the mean difference profiles from the vortex-average and trajectory matching analyses are included in the blue and red curves, respectively, in Figure 11. The result of these three independent approaches lead to generally consistent conclusions at the $\pm$ 5 % level, with mean difference profiles at most altitudes overlapping within their standard errors. However the vortex-average and trajectory matching results do not reproduce the POAM high bias between 12 and 17 km seen in the standard coincidence comparisons. In fact, it could be argued that these two approaches show a low POAM bias of a few percent, at least below 18 km. This discrepancy is not currently understood. Finally, we note that these results are generally consistent with the conclusions of *Danilin et al*. [2001], who have also done a systematic comparison of the POAM and ER-2 ozone measurements during SOLVE using both a trajectory hunting and direct coincidence analysis.

5. MkIV balloon comparisons

The Jet Propulsion Laboratory MkIV Interferometer [*Toon*, 1991] is a high-resolution Fourier transform infrared (FTIR) spectrometer. Like POAM, the MkIV makes measurements of atmospheric composition using the solar occultation technique, but operates in the infrared rather than the visible, and from a balloon rather than a satellite platform. In terms of optical design the MkIV is very similar to the ATMOS instrument [*Farmer*, 1987] which flew four times on the space shuttle. Following launch, the balloon rises to float altitude (typically 30 to 40 km) from which it then observes the Sun rise or set. When operating at high latitudes, such as during SOLVE, the sunrise/set transition is relatively slow, taking approximately two hours. During occultation, the instrument measures the solar radiance through the atmosphere in the spectral range from

650 to 5650 cm^{-1} (1.77 to 15.4 μm) at 0.01 cm^{-1} resolution. Normalization of the limb spectra by a high-Sun (unattenuated) spectrum removes the solar and instrumental features yielding atmospheric limb transmittance spectra. These transmittance spectra are analyzed using a nonlinear least squares spectral fitting algorithm to determine slant column abundances of various trace gases along the limb path from the depths of their absorption lines. Finally, the matrix equation relating the measured slant column abundances to the calculated slant path distances is solved to yield the final volume mixing ratio profiles for each gas. The MkIV retrieval algorithms are described by *Sen et al*. [1998]. The effective vertical resolution of the MkIV profiles is approximately 2 km. The accuracy of the ozone retrieval, which is determined primarily by uncertainties in spectroscopic parameters used in the line-by-line forward model, is estimated to be ~ 5 %.

The MkIV payload made two flights during SOLVE, launching from the Esrange balloon facility just outside of Kiruna. On the first flight, December 3 1999, MkIV measured a sunset occultation, whereas the second flight on March 15 2000 was a sunrise event. During the time it takes for the MkIV to record an occultation, the balloon can drift a significant distance horizontally, depending on the local wind fields. On each day POAM made two measurements close in latitude to the balloon position and bracketing it in longitude (see Figure 13 for details). The spatial separation between the balloon and satellite measurements is similar on both days, but the different character of the balloon track on the two flights introduces distinct differences. On the December flight the balloon drifted in a predominantly north-south direction and the two POAM measurements are almost equidistant in longitude from the MkIV and at the same average latitude. On the March flight the balloon traveled almost entirely in an east-west direction, bringing it in much closer spatial coincidence with one of the POAM measurements on that day. The temporal coincidence was also very different on the two flights. Because POAM measures local sunsets in the Northern Hemisphere, the two instruments made measurements in close temporal coincidence on the first date (MkIV sunset) but were separated by approximately 12 hours on the March flight (MkIV sunrise).

Another important difference between the two flights is the location of the measurements relative to the edge of the polar vortex. To look at this more closely we have plotted in Figure 12 profiles of equivalent latitude for the POAM and MkIV measurement locations, as well as the inner and middle vortex edges. The December 3 results in the left panel show POAM and MkIV sampling essentially identical equivalent latitudes well inside the inner vortex edge. On March 15, shown in the right panel, the situation is more complicated. The MkIV profile and the closest coincident POAM profile, at 39 E longitude, are fairly close in equivalent latitude and both just inside the vortex inner edge. The other POAM profile, at 14 E longitude, is clearly sampling different equivalent latitudes, more consistent with the middle of the vortex boundary.

In Figure 13 the POAM and MkIV ozone profiles are plotted for the two days. In both panels the black curve is the MkIV ozone and the blue and red curves correspond to the two coincident POAM profiles on each day. Both POAM profiles on Dec 3 show excellent overall agreement with the MkIV profile, deviating only at the very top of the profile, above 30 km. The March 15 results are also very satisfying. The POAM profile measured at 39 E, which we have seen is sampling coincident air masses with the balloon, reproduces the detailed vertical structure in the MkIV profile almost exactly, whereas the other POAM profile shows a very different vertical structure, consistent with fact that it is sampling very different air.

In Figure 14 we have plotted the ozone differences for each flight, calculated from equation (1). The two curves in each panel correspond to the two coincident POAM profiles on each date, with the red and blue curves having the same meaning as in Figure 13. On December 3 the differences are within 10 % with no obvious bias between 15 and 30 km, which is quite good. Above 30 km and below 15 km there is a systematic tendency for POAM to be biased high relative to MkIV. The disagreement is 10 – 20 % above 30 km and larger below 15 km, where it averages 20 % but reaches values as high as 30 % or more. The POAM satellite validation [*Rusch et al*., 2001] shows no evidence of a high bias in the version 3.0 ozone between 30 and 34 km. This is also not a known systematic bias of the MkIV instrument. However, it is useful to keep in mind that this is the upper limit of the MkIV retrieval range and the ozone retrievals at or near the balloon float altitude become very sensitive to assumptions about the shape of the O_3 profile above 33 km. These uncertainties are reflected in the larger MkIV error bars, which increase from < 0.1 ppm at 30 km altitude to ± 0.4 ppm at 34 km. Therefore the MkIV/POAM difference at these altitudes is probably not statistically significant.

For the March 15 flight the agreement between MkIV and the closest POAM measurement at 39 E is within 5 – 10 % at almost all altitudes. The exception is the 15 – 18 km region, where there is some mismatch in the small-scale structure seen in the two profiles, and the very lowest point at 12 km. Nevertheless, the overall agreement between these two profiles is very good, particularly when one keeps in mind the fact that the measurements were made almost 12 hours apart. As expected, the second POAM profile on this day does not agree with the MkIV nearly as well as the first above 15 km, with a very different vertical structure and differences in the ± 25 % range.

6. DOAS balloon comparisons

A single POAM measurement on February 18 2000 coincided with a balloon measurement made by the Laboratoire de Physique Molèculaire et Applications and Differential Optical Absorption Spectroscopy (LPMA/DOAS) instrument. The LPMA/DOAS balloon gondola was launched from Kiruna into the middle stratosphere and measured a suite of atmospheric trace gases including ozone. The LPMA/DOAS gondola carried two optical spectrometers (a DOAS and a FT-IR spectrometer) that analyze the direct UV-visible and near-IR part of the solar spectrum for line of sight (LOS) absorption - taken from the balloon gondola to the Sun - for a suite of atmospheric trace gases (for details of the measurement technique see, e.g., *Camy-Peyret et al.* [1993] and *Ferlemann et al.* [2000]).

The LPMA/DOAS gondola employs two kinds of observations, (1) measurements made through the atmosphere during balloon ascent for solar zenith angles typically smaller than 85^{o} and (2) solar occultation observed from balloon float altitude (~ 30 km). LOS ozone slant column density (LOS-SCD) is inferred by applying the DOAS technique to direct Sun spectra measured in the ozone Chappuis bands (495.2 - 618.2 nm). Ozone density profiles are then inferred from the measured LOS-SCD values using either the onion peeling, or the minimal estimate technique. For more details on the retrieval analysis see *Ferlemann et al*. [2000].

Taking into account the different spectrum integration times and spectral averaging, the vertical resolution of the measurements is as high as 100 m in ascent mode and 1 km in solar occultation mode. Absolute accuracy of the ozone retrievals is estimated to be 2.5 % in ascent mode and 2 % in solar occultation mode. Comparison of the DOAS ozone with *in-situ* measurements made by an electrochemical cell (ECC) on the same gondola agree within the range given by the uncertainty of the individual measurement (ECC accuracy ± 4 %, DOAS accuracy ± 2 %).

Only one POAM measurement was close enough to the balloon position on this day to give a reasonable coincidence. Like POAM, the balloon measured a sunset occultation on this flight and therefore the temporal coincidence is quite good between POAM and the DOAS occultation measurement (the time of the DOAS ascent measurement, on the other hand, precedes the POAM measurement by 2 – 3 hours). To quantify the measurement positions relative to the vortex edge, Figure 15 shows the equivalent latitude profiles calculated for the DOAS and POAM locations from the UKMO PV fields. The solid and dashed-dotted blue curves represent the DOAS occultation and ascent profiles, respectively, and the solid red curve is the POAM profile. The dashed and dotted black profiles represent the equivalent latitude of the middle and inner vortex edges, respectively.

These results show that both DOAS measurements occur inside the inner vortex edge at all altitudes except perhaps at the very bottom of the profile. Above 23 km the ascent and occultation profiles coincide but below that the ascent measurement samples higher equivalent latitude than the occultation. The POAM measurement is also coincident in equivalent latitude with DOAS, and therefore inside the inner vortex edge, above 22 km but samples lower equivalent latitudes than either of the DOAS profiles at lower altitudes. Due to the proximity to the vortex edge one might expect a fairly complicated situation, with significant horizontal gradients in the ozone. In particular it is interesting to note that the POAM and DOAS measurements happen to straddle the Scandinavian mountains. The LPMA/DOAS probed air masses in the very lee of the mountain range (with the ascent measurements more eastward than the occultation measurements) whereas POAM probed air masses mostly westward (upwind) from the mountains. Hence a pronounced dynamical disturbance of the ozone field is probably to be anticipated.

In Figure 16 the POAM ozone profile is plotted in the black curve along with the DOAS ascent and occultation profiles in the blue and red curves, respectively. There is good qualitative agreement between the three profiles. In particular the distinct notch structure in the peak of the ozone profile is well captured by both POAM and DOAS, although the altitude of this structure is more consistent between the POAM and DOAS/occultation profiles than the DOAS/ascent. Another feature captured well by all three measurements is the small positive inflection in the profile between 19 and 25 km, which in this case is more consistent in the POAM and DOAS/ascent data. It is also impressive how well the DOAS profiles track the POAM profile all the way down to its lowest point at 9 km.

The ozone difference profiles are plotted in Figure 17. The difference is calculated from equation (1) after first interpolating the DOAS data onto the standard POAM altitude grid (the DOAS ascent data have already been smoothed to a 1-km resolution consistent with POAM). The POAM and DOAS occultation profiles essentially agree to within 10 % at all altitudes between 10 and 30 km. However there appears to be a fairly systematic bias in the differences, with POAM generally lower than DOAS by 3 – 5 % from 11 to 18 km, increasing to 5 – 8 % from 18 to 29 km. The POAM and DOAS ascent differences, on the other hand, appear to be zero-mean with no significant bias. However, the scatter in the difference profile does show strong altitude dependence, with absolute differences less than 5 % between 20 and 30 km but increasing to 20 % below 15 km. Altogether these comparisons are remarkably good given the expected natural atmospheric variability in the ozone near the vortex edge.

7. OMS/JPL Ozone comparisons

The JPL balloon-borne *in situ* ozone instrument is virtually identical to the ozone instrument on the ER-2 aircraft. Ozone is measured in two chambers, one containing unperturbed air, the other containing air scrubbed of ozone. The ratio of the absorption of 254-nm radiation (generated by a single mercury lamp) in the two chambers is measured simultaneously, canceling out lamp intensity fluctuations. This ratio, coupled with the well-known O_3 absorption cross-section and the temperature (controlled and easily measured), pressure, and path length of the chambers is used to determine the mixing ratio of O_3 in ambient air. The mixing ratio of O_3 is measured every second with an overall uncertainty (accuracy plus precision) of 3 to 5%. Pressure is measured with a set of calibrated Baratrons with an accuracy of 1%. On the Observations of the Middle Stratosphere (OMS) balloon flights, *in situ* measurements are obtained on slow ascent (300 meters/minute) to 8 mb, a float of about 20 minutes, and a slow descent (150 meters/minute) through most of the stratosphere, followed by a rapid descent on a parachute.

The JPL Ozone instrument flew on two OMS balloon flights launched from Esrange during SOLVE, on November 19 1999 and March 5 2000. *Salawitch et al.* [2001] use the data to quantify ozone loss in the vortex, and provide a discussion of the location of the balloon flights and comparisons to MkIV remote measurements as well as ER-2 NOAA Ozone data. Both OMS flights sampled air deep in the vortex. Unfortunately POAM was not operating on November 19 (due to a safety shutdown for the Leonid meteor shower) and therefore a direct coincidence with this OMS flight does not exist. However, POAM did make a measurement very close to Esrange on the following day (November 20) and this profile has been used as a basis for the POAM/OMS comparison for the November flight. For the March 5 OMS flight a good spatial and temporal coincidence with POAM does exist.

Panels (a) and (b) of Figure 18 show the comparison between POAM and the JPL *in situ* ozone data for the two flights. The natural vertical coordinate for the JPL Ozone measurements is pressure, which is measured directly by the instrument as described above. Since the fundamental POAM vertical grid is geometric altitude, we have used the UKMO pressure profile (collocated with the time and location of the POAM measurement) to convert the POAM ozone profile to a pressure grid for the sake of these comparisons. In these plots the red profile represents the POAM measurement and the blue dots represent the entire OMS measurement profile (i.e., ascent and descent phases). In both cases the agreement is excellent, and rivals that seen for *in situ* - remote comparisons of instruments flying on the same balloon gondola [*Sen et al.,* 1998].

Even though the two measurements are made a day apart, the November comparison shown in Figure 18 (a) is interesting because the excellent agreement confirms the very low ozone abundances seen for deep vortex air (~ 3 ppm for altitudes above 50 mb). As discussed in *Salawitch et al.* [2001], this relatively low abundance reflects normal gas phase chemistry under conditions of low solar illumination: the shorter wavelengths which produce ozone are absent, but slightly longer near-UV wavelengths which drive photochemical destruction processes are still present. The "notch" in the balloon profile around 25 mb is a real atmospheric feature, seen in both the ascent and descent measurements from the balloon. The lower ozone in the notch may simply reflect different air parcel trajectory history with different solar illumination, and may be an indicator of variability, on at least small scales, of ozone in the newly forming vortex. Since POAM should be capable of resolving a feature of this vertical scale, the fact that it is not evident in the POAM profile suggests that the notch itself is indeed a localized feature, which does not recur at the time and location of the POAM measurement (although the ozone abundance measured by POAM is midway between the lower amount of the notch and the surrounding air).

The good agreement of balloon and POAM low ozone in the mid- to upper-stratosphere for observations separated in space and time suggests that these abundances are representative of a significant portion of the core of the vortex. Since this is air that will later descend to PSC-induced ozone loss altitudes, the low initial abundances of ozone have implications for calculations of ozone loss. Also, even though much of the vortex core is in darkness, displacements to lower latitudes afford an opportunity for a solar occultation instrument such as POAM to obtain vortex core measurements, which can be used for calculations of vortex average ozone loss with appropriate data filtering and selection (see *Hoppel et al*. [2001]).

For the sake of quantitative comparison, we focus on the March 5 flight, where the OMS and POAM observations were coincident within 1 degree in latitude, 10 degrees in longitude and 2 hours in time. The results, shown in Figure 18 (b), show excellent agreement overall in both the magnitude and vertical structure of the ozone profile. The ability of POAM to discern the very steep falloff in ozone near 30 mb is especially noteworthy and demonstrates the capability of the instrument to resolve sharp vertical structures. The ER-2 NOAA Ozone data for this date also lie on top of the JPL balloon data for the 50-100 mb region (see Figure 5 of *Salawitch et al*. [2001]). Combined with the POAM/ER-2 direct comparison on this date (see Figure 10) these results illustrate the good overall agreement between POAM and *in situ* measurements.

Figure 18c shows the relative difference profile as a function of altitude. To calculate this profile, the JPL data were first binned in $\ln(\mathrm{pressure})$ then interpolated to altitude using the POAM/UKMO pressure profile. The difference was then calculated according to Equation (1). The difference is within 10 %, and often less than 5 %, from 13 to 29 km, but increases to approximately 18 % at the very lowest altitude of 11 km. Ozone is quite variable in the lower stratosphere, and variations this large are seen in the JPL Ozone data itself there. In spite of the generally good quantitative agreement it is obvious that there is a bias in the difference, with POAM higher than JPL Ozone by 3-5 % on average above 12 km. We considered the possibility that this bias is introduced by errors in the transformation between pressure and altitude grids. However, the UKMO and JPL Ozone pressure profiles are in good agreement and the use of an alternate scheme to calculate the differences, in which the JPL measurements are compared directly to POAM in altitude space using the onboard GPS altitude determination from the OMS gondola, yielded essentially identical results.

It is quite possible that the difference between the OMS and POAM ozone simply reflects real atmospheric variation for these close, but still separated, measurements. The differences seen in March between OMS and POAM are not outside the atmospheric variability, for example, as seen in November between 25-50 mb in the ascent and descent data from OMS. This suggests that even over the scale of the balloon flight, there were real atmospheric differences in the vertical profiles of ozone. It is not possible with only a single comparison to identify the exact cause of the apparent 3-5% bias between POAM and JPL Ozone, although it is certainly within the instrumental uncertainties, as well as reasonable atmospheric variability, especially when the very different nature of the instruments' spatial sampling is considered.

8. SAOZ balloon comparisons

The Système D'Analyse par Observations Zénithales (SAOZ) sonde is a lightweight UV-visible diode array spectrometer that measures the absorption of sunlight by the atmosphere during the ascent (or descent) of the balloon and during sunset (or sunrise) from float altitude. A simple conical mirror replaces the gondola orientation or sun tracker systems generally used on large balloon platforms. The balloon version of the SAOZ instrument is very similar to the one used for ground-based measurements of total ozone and NO_2 [*Pommereau et al.,* 1988]. It is a commercial flat field, 360 grooves/mm, holographic grating spectrometer equipped with a 1024-diode linear array and an entrance slit of 50 µm. In this arrangement, measurements are made between 290 and 640 nm, with an average resolution of 0.8 nm. Ozone is measured in the visible from 450 to 620 nm, where its absorption cross-section is relatively insensitive to temperature. The SAOZ is equipped with a Global Positioning System (GPS) receiver, which allows its location to be determined in three dimensions with an uncertainty of ± 150 m.

The spectral analysis and the inversion scheme used for SAOZ are discussed in *Pommereau et al*. [1994]. The inversion assumes the scattered light component to be negligible, an important point because of the use of a 360° conical mirror plus diffuser instead of a tracker. The random error in the retrieved ozone profiles varies from 0.1% at 30 km to 1 - 2 % at 11 km. Including the maximum expected cross section errors (1%) and errors in the reference spectrum used in the spectral analysis (0.5%), the total accuracy of the SAOZ ozone (random + systematic) ranges from approximately 1.5 % at 30 km to 3.4 % at 11 km. The vertical resolution of the measurements is 1.4 km and the data are sampled at 1-km intervals.

As part of the THESEO 2000 campaign SAOZ instruments made eight flights from Kiruna in Sweden (68 N, 21 E) or Andoya in Norway (69 N, 16 E) during the 99/00 winter. All of the SAOZ balloon launches were made at local sunset and thus coincide closely in time with the POAM measurements (generally within one hour). In selecting SAOZ data to compare with POAM we allow for the fact that the SAOZ measurement events can cover a significant horizontal distance due to the balloon drift. We therefore search for POAM coincidences among the SAOZ ascent and occultation measurements independently on each day. For the comparisons shown here we have adopted a separation criteria of ± 2 degrees in latitude and ± 4 degrees in longitude. Using this criteria there are coincidences with POAM on five days: the Andoya flight on Nov 17 and the Kiruna flights on January 28, February 27, March 7 and March 25. On February 27 and March 25 only one of the two SAOZ measurements (the occultation and ascent profiles, respectively) satisfied the coincidence criteria. On all other days both SAOZ profiles are retained. Despite the stated coincidence criteria, almost all of these SAOZ measurements occur within 1 degree in latitude and 3 degrees longitude of the POAM tangent point.

Both the SAOZ and POAM measurements occurred well within the polar vortex on all these days except for February 27, where the measurements coincided with the inner vortex edge, and March 25, where both measurements were well outside the vortex. Figure 19 shows the comparison of the POAM and SAOZ ozone profiles on each of these days. The black curve represents the POAM profile, while the blue and red curves are the SAOZ ascent and occultation measurements, respectively. For the most part, the agreement shown in Figure 19 is very good. Often the SAOZ ascent and occultation profiles show different vertical structure in the profile, indicating a significant amount of atmospheric variability even over the temporal and spatial scales spanned by the balloon measurement. The only notable exception to the good agreement between the two instruments is the February 27 coincidence, where POAM appears to be systematically low with respect to the SAOZ occultation profile. While these two measurements are made in close spatial proximity, as noted previously this is the only occasion where both POAM and SAOZ are sampling near the vortex edge instead of well inside or outside the vortex. One might therefore expect a greater degree of natural spatial variability in the ozone field in this situation

Figure 20 shows the mean POAM/SAOZ ozone difference profile, calculated by averaging over all coincident ascent and occultation profiles shown in Figure 19. Between 14 and 27 km the absolute difference is within 5 - 7 % everywhere, however POAM appears to be biased low compared to SAOZ by 2 – 3 % on average. Below 14 km POAM is high relative to SAOZ, with differences increases to a maximum of ~ 20 % at 10 km.

9. Summary and conclusions

A summary of the POAM ozone comparisons made in this paper is shown in Figure 21. Here we have only used comparisons that were obtained either completely in or completely out of the vortex. Measurements made near the edge of the vortex were discarded because of the possibility of large horizontal gradients in the ozone, which can significantly complicate interpretation of the results. Thus, we have eliminated the DC-8 comparisons obtained on March 9, and have also eliminated the low altitude (< 15 km) portions of the January 16 and March 3 DC-8 coincidences. For the ER-2 comparisons, we have used the direct coincidence comparisons discussed in Section 4.3 because they cover the largest altitude range. For the MkIV comparisons we have averaged the differences obtained from the two coincident profiles on December 3, as well as the single coincidence at 39 E on March 15, which we feel is a valid coincidence despite the vortex edge conditions (see Figure 12 and accompanying discussion). For the POAM/DOAS summary we have averaged the differences from the DOAS occultation and ascent profiles. Again, we feel these comparisons are valid in spite of their proximity to the vortex edge, based on the arguments made previously. The OMS result comes from the single coincidence on March 5 2000 and is identical to the result shown in

Figure 18c. Finally, the SAOZ profile is obtained by averaging all the coincidences shown in Figure 19 except for the February 27 event, which occurred at the vortex edge as discussed in Section 8.

The comparisons shown in Figure 21 naturally divide into 3 altitude regions: below 14 km, 14-30 km, and above 30 km. In the primary altitude range between 14 and 30 km, where the majority of the coincident measurements are made and the statistics are therefore the best, POAM agrees with all the SOLVE data sets examined in this paper to within 7-10 % with no apparent bias (this conclusion ignores the divergence with UV DIAL above 20 km, which is explained in section 3.3, and the peak in the POAM/AROTEL difference at 28-29 km, which is dominated by a single bad comparison on December 2). The observed differences are within the combined errors of POAM and the correlative measurements in this altitude range and collectively demonstrate an impressive degree of consistency between the various datasets, despite the very different measurement techniques and spatial sampling inherent in the data. These differences are also consistent with the POAM satellite and ECC sonde validation in this altitude range [*Rusch et al.,* 2001].

Below 14 km there is a great deal of scatter in the SOLVE comparisons. The most extensive comparisons come from the ER-2 measurements, which indicate a high POAM bias (~ 20 %) at the lower altitudes, but only below 10 km. The SAOZ and MkIV comparisons also tend to show POAM biased high by 10–20 % below 14 km. However the UV DIAL, DOAS, and JPL/OMS comparisons, while exhibiting larger differences in this altitude range (± 15 %), show no consistent bias. Validation of the POAM version 3.0 ozone with satellites and ECC sondes does indicate a high bias in the Northern

Hemisphere below 14 km but the magnitude is somewhat uncertain, ranging from 5 to 25% at 10 km [*Rusch et al.,* 2001]. In summary, it is difficult to evaluate the consistency of the SOLVE comparisons in this altitude range with previous comparisons, and the actual POAM accuracy remains somewhat uncertain.

Above 30 km there are only the AROTEL and MkIV comparisons, both of which seem to suggest a high POAM bias in this altitude range. However, there is a large amount of scatter in these results, which are based on only 4 measurements (the AROTEL coincidences on December 14 and March 9 and the two MkIV coincidences on December 3). It is worth noting that comparisons with HALOE and SAGE II do not rule out the possibility of a high POAM bias between 30 and 35 km, but the magnitude of the discrepancy is no more than 5 % in the satellite comparisons [*Rusch et al.,* 2001]. Therefore, we feel that the SOLVE comparison results are inconclusive above 30 km.

In conclusion, the SOLVE campaign has provided abundant opportunities for validating POAM ozone. This is especially true in the 14 - 30 km region. In this altitude range the comparisons with all seven correlative data sets considered in this study are remarkably consistent, and indicate agreement to well within the expected uncertainties in POAM ozone obtained both from formal error analysis [*Lumpe et al.,* 2001] and other validation studies [*Rusch et al.,* 2001]. However, the situation is not as clear-cut below 14 km or above 30 km where few measurements and large scatter complicate the comparisons. The altitude region above 30 km is not an important issue because it is very clear that, in this altitude range, ozone can be measured very well from satellites, and validation opportunities (apart from those obtained in dedicated campaigns) abound. The altitude region below 14 km is much more important. In this region, for a variety of reasons, ozone is much more difficult to measure by satellite-based instruments, and the accuracy of these measurements is not very clear. However, long-term data sets provided by satellites in this altitude region have significant scientific value, so their reliability must be carefully assessed. Obtaining a large number of high-precision measurements in this altitude region should be a very high priority in the planning of future satellite validation campaigns.

Acknowledgments

This work was supported by the NASA Scientific Data Purchase program through contract # NAS13-99031. The version 3.0 POAM data are archived at the NASA Langley Research Center EOSDIS Distributed Active Archive Center. We wish to thank Ross Salawitch for his work in making the entire ER-2 data set available in a very convenient form in terms of his “merge files”.

The balloon experiments have been operated by the teams of the NASA National Scientific Balloon Facilites (NSBF), the Centre National d'Etude Spatiales (CNES), the Swedish Space Corporation (SSC) and the Norwegian Space Center (NSC) which are gratefully acknowledged. European SAOZ and LPMA/DOAS experiments were supported by the EC Environmental Programmes THESEO-Eurosolve EVK2-1999-00311 and Alomar LSF.

References

Browell, E. V., Differential absorption lidar sensing of ozone, Proc. IEEE, 77, 419-432, 1989.

Browell, E. V., C. F. Butler, S. Ismail, M. A. Fenn, S. A. Kooi, A. F. Carter, A. F. Tuck, O. B. Toon, M. H. Proffitt, M. Loewenstein, M. R. Schoeberl, I. Isaksen, and G. Braathen, Airborne lidar observations in the wintertime Arctic stratosphere: Ozone, Geophys. Res. Lett., 17, 325-328, 1990.

Browell, E. V., C. F. Butler, M. A. Fenn, W. B. Grant, S. Ismail, M. Schoeberl, O. B. Toon, M. Loewenstein, and J. R. Podolske, Ozone and aerosol changes observed during the 1992 Airborne Arctic Stratospheric Expedition, Science, 261, 1155-1158, 1993.

Browell, E. V., S. Ismail, and W. B. Grant, Differential absorption lidar (DIAL) measurements from air and space, Appl. Phys. B 67, 399-410, 1998.

Camy-Peyret, C., Flaud, A. Perrin, C.P. Rinsland, A. Goldman, and F. Murcray, Stratospheric N_2O_5, CH_4, and N_2O profiles from IR solar occultation spectra, J. Atmos. Chem., 16, 31 - 40, 1993.

Danilin, M. Y., et al., Comparison of ER-2 aircraft and POAM III, MLS, and SAGE II satellite measurements during SOLVE using traditional correlative analysis and trajectory hunting technique, submitted to *J. Geophys. Res*, 2001.

Farmer, C. B., High-resolution infrared spectroscopy of the Sun and the Earth's atmosphere from space, *Microchim. Acta [Wien], III*, 189-214, 1987.

Ferlemann, F., N. Bauer, R. Fitzenberger, H. Harder, H. Osterkamp, D. Perner, U. Platt, M. Schneider, P. Vradelis, and K. Pfeilsticker, Differential Optical Absorption

Spectroscopy Instrument for stratospheric balloon-borne trace gas studies, Applied Optics, 39, 2377 - 2386, 2000.

Grant, W. B., M. A. Fenn, E. V. Browell, T. J. McGee, U. N. Singh, M. R. Gross, I. S. McDermid, L. Froidevaux, and P.-H. Wang, Correlative stratospheric ozone measurements with the airborne UV DIAL system during TOTE/VOTE, *Geophys. Res. Lett.*, 25, 623-626, 1998.

Hoppel, K. et al., POAM III observations of Arctic ozone loss for the 1999/2000 winter, submitted to *J. Geophys. Res.*, this issue, 2001.

Lucke, R.L., *et al*., The Polar Ozone and Aerosol Measurement (POAM) instrument and early validation results, *J. Geophys. Res,* 104, 18,785-18,799, 1999.

Lumpe *et al*., POAM III retrieval algorithm and error analysis, submitted to *J. Geophys. Res.*, 2001.

McGee, T. J., M. Gross, U.N. Singh, J. J. Butler, and P. Kimvilakani, "An Improved Stratospheric Ozone Lidar", Opt. Engin., 34, 1421-1430, 1995.

McGee, T. J., J. F. Burris, L. Twigg, D. Silbert, W. Heaps, W. Hoegy, G. Sumnicht, C. Hostetler, G. Hansen, P. Lucker, M Osborne, M Lawrence, R. Neuber and T. Schmidt, The AROTEL Instrument - an airborne lidar for stratospheric ozone, aerosols and temperature, submitted to Applied Optics, 2001.

Nash, E. R., P. A. Newman, J. E. Rosenfield, and M. R. Schoeberl, An objective determination of the polar vortex using Ertel's potential vorticity, *J. Geophys. Res.*, 101, 9471-9478, 1996.

Pommereau, J. P. and J. Piquard, Ozone, nitrogen dioxide and aerosol vertical distributions by UV-visible solar occultation from balloons, *Geophys. Res. Lett*, 21, 1227-1230, 1994.

Pommereau, J.P. and F. Goutail, O_3 and NO_2 ground-based measurements by visible spectrometry during Arctic Winter and Spring 1988, *Geophys. Res. Lett*, 891, 1988.

Proffitt, M. H., et al., In situ ozone measurements within the1987 Antarctic ozone hole from a high-altitude Er-2 aircraft, *J. Geophys. Res.*, 94, 16,547-16,555, 1989.

Randall, C.E., R.M. Bevilacqua, J.D. Lumpe, K.W. Hoppel, D.W. Rusch, and E.P. Shettle, Comparisons of Polar Ozone and Aerosol Measurement (POAM) II and Stratospheric Aerosol and Gas Experiment (SAGE) II aerosol measurements from 1994 to 1996, *J. Geophys. Res.* 105, 3929-3942, 2000.

Randall, C.E., R.M. Bevilacqua, J.D. Lumpe and K.W. Hoppel, Validation of POAM III aerosols: Comparison to SAGE II and HALOE, Validation of POAM Aerosols: Comparison to HALOE and SAGE II, submitted to *J. Geophys. Res.*, 2001a.

Randall C. E. et al., Construction of 3D Ozone Fields Using POAM During SOLVE, submitted to *J. Geophys. Res.*, this issue, 2001b.

Rusch et al, "Validation of POAM II Ozone Measurements with Coincident MLS, HALOE, and SAGE II Observations", *J. Geophys. Res.*, 102, 23,615-627, 1997.

Rusch, D.W., et al., Validation of POAM III O3: Comparison to ozonesonde and satellite data, submitted to *J. Geophys. Res.*, 2001.

Salawitch, R. J., J. J. Margitan, B. Sen, G. C. Toon, G. B. Osterman, M. Rex, J. W. Elkins, E. A. Ray, F. L. Moore, D. F. Hurst, P. A. Romashkin, R. M. Bevilacqua, K. Hoppel, E. C. Richard, and T. P. Bui, "Chemical Loss of Ozone During The Arctic

Winter of 1999-2000: An Analysis Based on Balloon-borne Observations", submitted to *J. Geophys. Res*., this issue, 2001.

Sen, B., G. C. Toon, G. B. Osterman, J.-F. Blavier, J. J. Margitan, R. J. Salawitch, and G. K. Yue, Measurements of reactive nitrogen in the stratosphere, *J. Geopys. Res*., 103, 3571-3585, 1998.

Toon, G. C., The JPL MkIV Interferometer, *Opt. Photonic News*, 2, 19-21, 1991.

Figure Captions

Fig. 1 Comparison of the POAM (solid line) and predicted SAGE III (dashed line) Northern Hemisphere measurement latitudes during the year. For POAM this is invariant from year to year. The SAGE III ephemeris will likely change slightly depending on exact launch date and time.

Fig. 2 Locations of the POAM and DC-8 coincidences for six DC-8 flights. The blue line on each map represents the DC-8 flight track. The red circle is the location of the POAM measurement for which the coincidence comparisons are made. It is surrounded by a red rectangle that represents the area defined by the coincidence criteria ($\pm$1 deg latitude, $\pm$2 deg longitude). Black contours (solid, dashed, solid) represent the vortex inner, middle and outer edge, respectively, on the 450 K potential temperature surface.

Fig.3 POAM (black), UV DIAL (red) and AROTEL (blue) ozone profiles measured during the six coincidence periods shown in Figure 2. The POAM curves correspond to the single profile measured at the location represented by the red circle in Figure 2. All UV DIAL and AROTEL data meeting the coincidence criteria for each flight have been averaged to produce the single profile shown here.

Fig. 4 Ozone difference, as calculated by equation (1), for POAM/UV DIAL (top panel) and POAM/AROTEL (middle panel). Blue and red curves represent the difference profiles for each of the 6 flights, whereas the black curve is the mean difference of all flights. Error bars correspond to the standard error of the mean difference. The bottom panel simply compares the POAM/UV DIAL and POAM/AROTEL mean error profiles from the top two panels.

Fig. 5 Examples of POAM and ER-2 data used in the vortex-averaged ozone comparisons for 4 ER-2 flights. The blue curves correspond to the ER-2 flight track on each day. The black and green contours represent the location of the inner and middle vortex edge, respectively, on the 450 K potential temperature surface. Red circles show the location of all POAM measurements made in the three-day period centered on the ER-2 flight date. Only those POAM and ER-2 measurements made inside the black contour are used in the vortex average comparisons.

Fig. 6 Vortex-average ozone mixing ratio profiles measured by POAM (red circles) and ER-2 (black squares) for the 11 ER-2 flights indicated at the top of each panel. The solid black and red lines represent the standard error of the means for POAM and ER-2, respectively.

Fig.7 POAM (red circles) and ER-2 (black triangles) ozone measurements at 460 K on Jan 23 (top panel) and March 11 (bottom panel). The POAM data include all measurements made within $\pm$ 1 day of flight date. Only in-vortex ER-2 data are plotted. The vertical lines denote the middle and inner vortex edges.

Fig. 8 The left panel shows the POAM and ER-2 in-vortex ozone mixing ratio profile averaged over all 11 ER-2 flights shown in Figure 6 (symbols are the same as in Figure 6). The right panel shows the mean ozone difference profile for the 11 flights. Error bars represent the standard error of the mean difference.

Fig. 9 Results of the trajectory matching analysis for 11 ER-2 flights. Black dots represent the ozone difference for all trajectory parcels that satisfy the coincidence criteria outlined in section 4.2. There are 249 such matches. The black curve is the mean difference at each potential temperature level and error bars represent the standard error of the mean difference.

Fig.10 POAM (blue) and ER-2 (red) ozone mixing ratios satisfying the coincidence criteria on each of 10 ER-2 flights. The coincidence criteria used are ± 3 deg latitude, ± 10 deg longitude and ± 3 hours. The POAM profiles represent the single coincident measurement from each day. The ER-2 profiles are constructed by binning all coincident ER-2 data for each flight into 1-km altitude bins.

Fig. 11 Summary of POAM /ER-2 ozone differences obtained from three comparison techniques. The black curve represents the mean difference obtained from the POAM/ER-2 direct coincidences on the 10 flights shown in Figure 10. The number of coincident ER-2 data points at each altitude level is shown at the right edge. For comparison the blue and red curves are the mean differences from the vortex-averaging and trajectory matching analyses, respectively (see Figures 8 and 9). These have been interpolated to an altitude grid using a mean vortex-averaged potential temperature profile. In all cases the error bars represent the standard error of the mean difference.

Fig. 12 Equivalent latitude profiles for the coincident POAM (red) and MkIV (blue) ozone measurements made on Dec 3 1999 and March 15 2000. For comparison the equivalent latitude of the inner and middle vortex edges are plotted in the black curves.

Fig. 13 Coincident ozone mixing ratio profiles measured by MkIV (black curves) and POAM (blue and red curves) on Dec 3 1999 and March 15 2000. The two POAM profiles correspond to the two closest measurements to the balloon position on each day.

Fig.14 Ozone difference profiles (from equation (1)) for the POAM /MkIV coincidence measurements shown in Figure 13. For each day the red and blue curves represent the difference between MkIV and the POAM profile of the same color in Figure 12.

Fig. 15 Equivalent latitude profiles for the coincident POAM (red) and DOAS (blue) ozone measurements made on February 18 2000. For comparison the equivalent latitude of the inner and middle vortex edges are plotted in the black curves.

Fig. 16 Coincident ozone density profiles measured by POAM (black curve) and DOAS ascent mode (blue curve) and occultation mode (red curve) on February 18 2000.

Fig. 17 Ozone difference profiles (from equation (1)) for the POAM /DOAS coincidence measurements shown in Figure 16. The red and blue curves represent the difference between the POAM measurement and the DOAS occultation and ascent measurements, respectively.

Fig. 18 Panel (a) shows the ozone mixing ratio profile measured by the JPL Ozone instrument on November 19 2000 in the blue symbols. The red curve represents the ozone measured by POAM on November 20 at approximately the same location (see figure legend for exact measurement locations). Panel (b) shows coincident ozone mixing ratio measurements made by POAM (red curve) and JPL Ozone (blue symbols) on March 5 2000. Panel (c) represents the ozone difference profile calculated for the March 5 2000 coincidence.

Fig. 19 Ozone density profiles measured by POAM (black curve) and SAOZ ascent mode (blue curve) and occultation mode (red curve) for coincident events on five different days. The coincidence criteria used are discussed in Section 8. The locations of the measurements are listed in the legend, with the text color chosen to correspond to the ozone profiles.

Fig. 20 Mean ozone difference profile (from equation (1)) for the POAM /SAOZ coincidence measurements shown in Figure 20. Error bars correspond to the standard error of the mean difference.

Fig. 21 Summary comparison of ozone difference between POAM and AROTEL (solid blue), UV DIAL (solid red), ER-2 (solid green), MkIV (black), DOAS (dashed blue), OMS (dashed red) and SAOZ (dashed green). All profiles represent the mean difference calculated from equation (1). Only coincident measurements obtained either completely in or completely out of the vortex are used to calculate these final difference profiles, as discussed in Section 9.

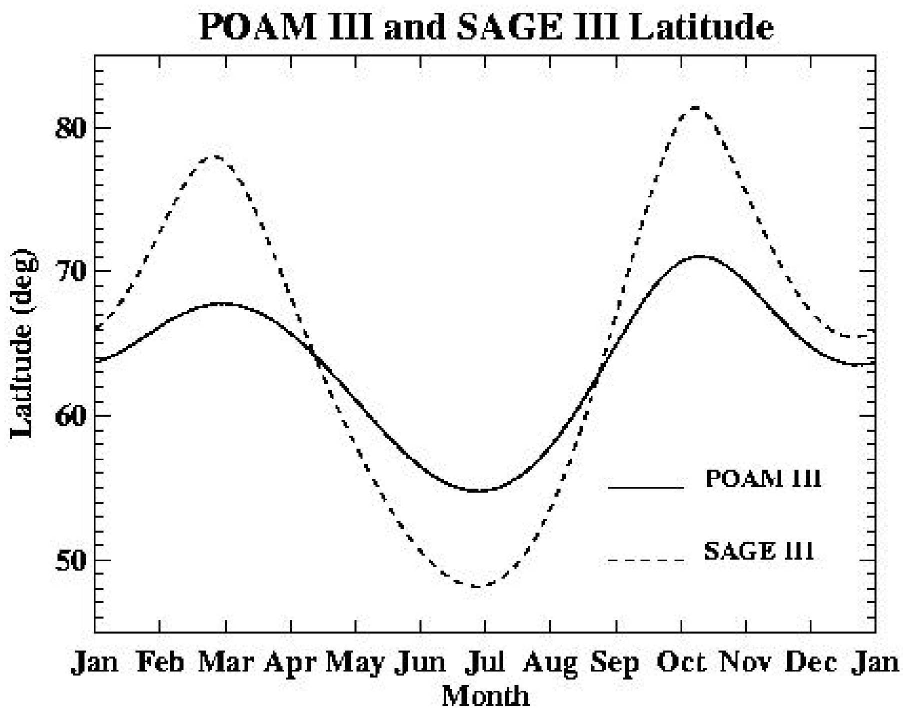
POAM III and SAGE III Latitude
80
70
60
50
Latitude (deg)
POAM III
SAGE III
Jan Feb Mar Apr May Jun Jul Aug Sep Oct Nov Dec Jan
Month

Figure 1

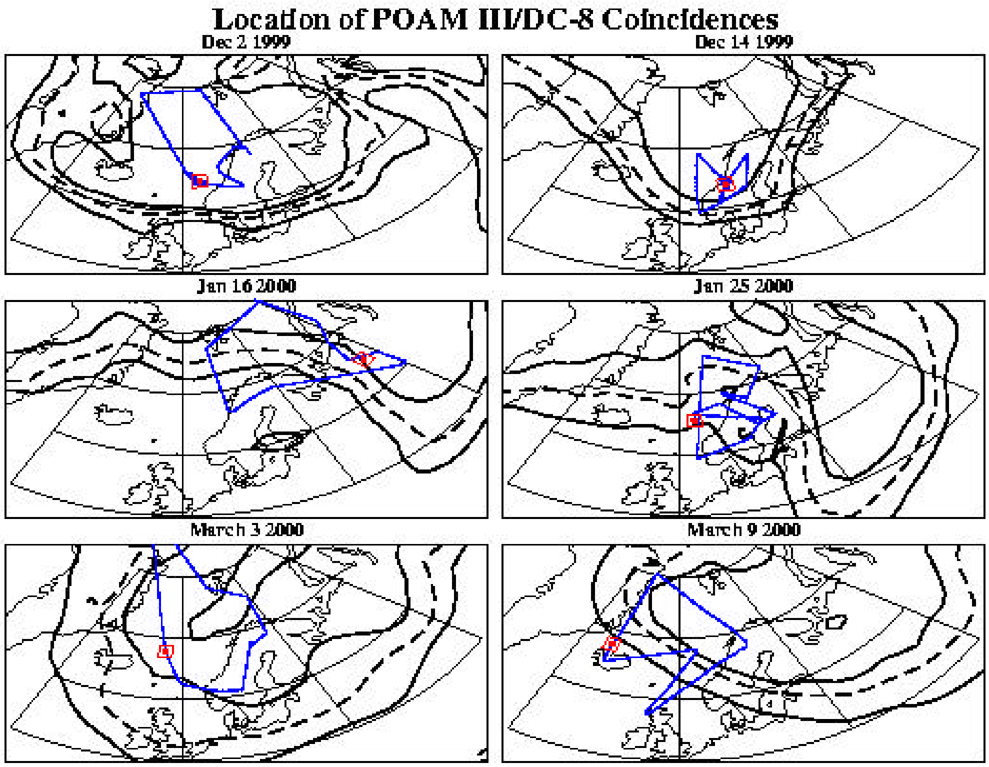
Location of POAM III/DC-8 Coincidences
Dec 2 1999
Dec 14 1999
Jan 16 2000
Jan 25 2000
March 3 2000
March 9 2000

Figure 2

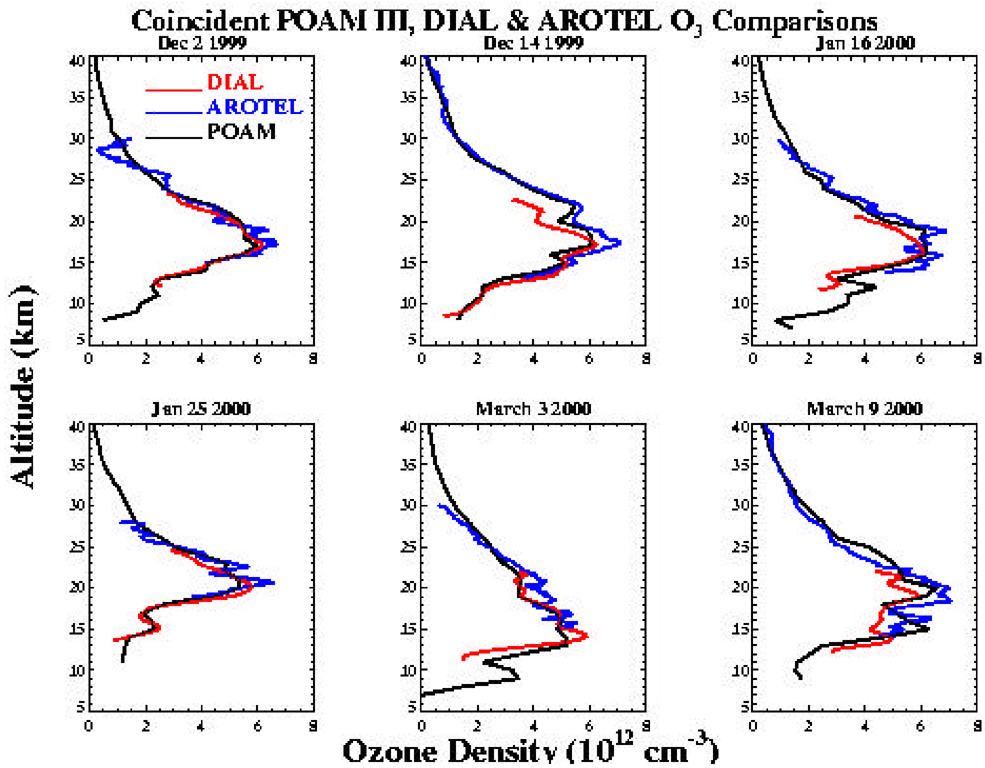
Coincident POAM III, DIAL & AROTEL O3 Comparisons
Dec 2 1999
Dec 14 1999
Jan 16 2000
Jan 25 2000
March 3 2000
March 9 2000
DIAL
AROTEL
POAM
Altitude (km)
Ozone Density (10^12 cm^-3)

Figure 3

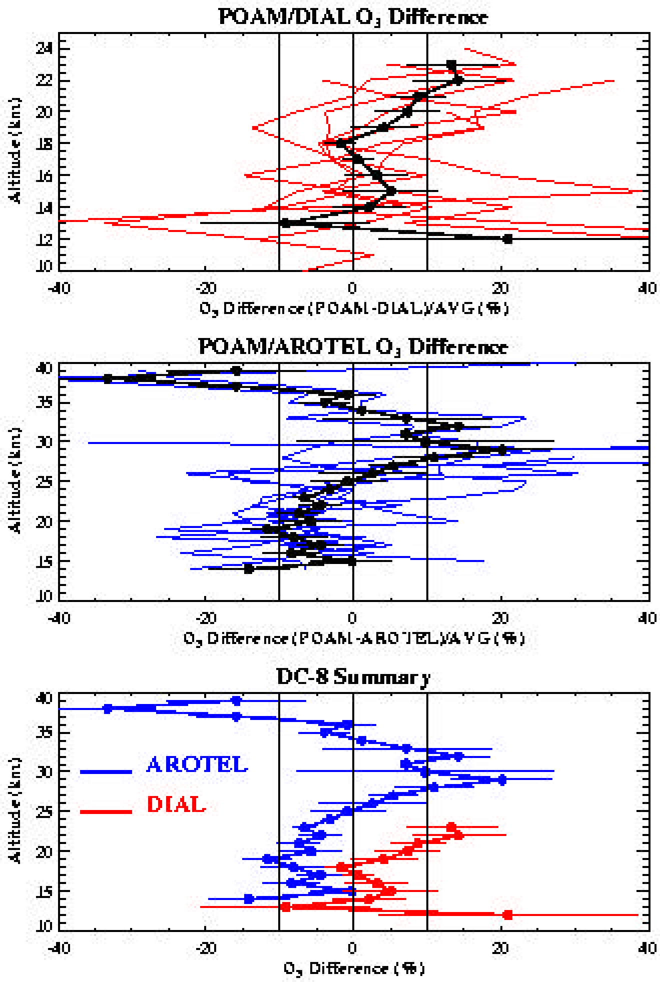

POAM/DIAL O3 Difference
Altitude (km)
O3 Difference (POAM-DIAL)/AVG (%)
POAM/AROTEL O3 Difference
Altitude (km)
O3 Difference (POAM-AROTEL)/AVG (%)
DC-8 Summary
AROTEL
DIAL
Altitude (km)
O3 Difference (%)

Figure 4

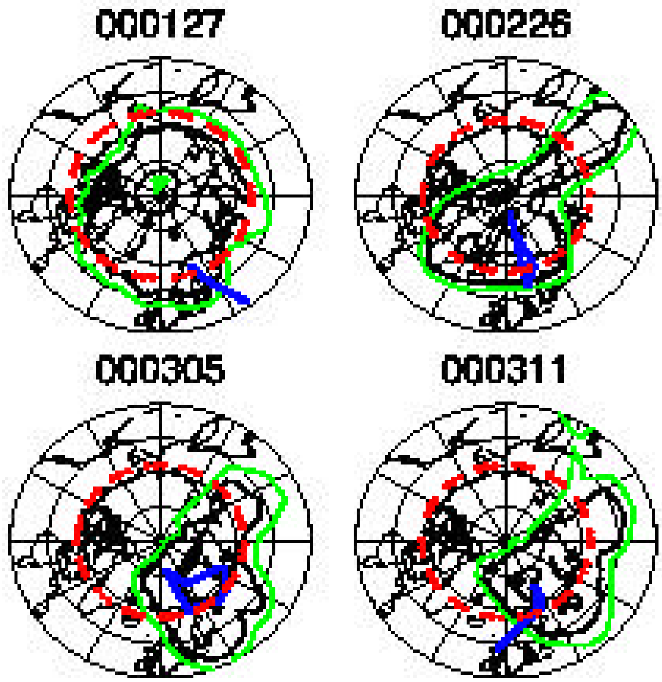

Figure 5

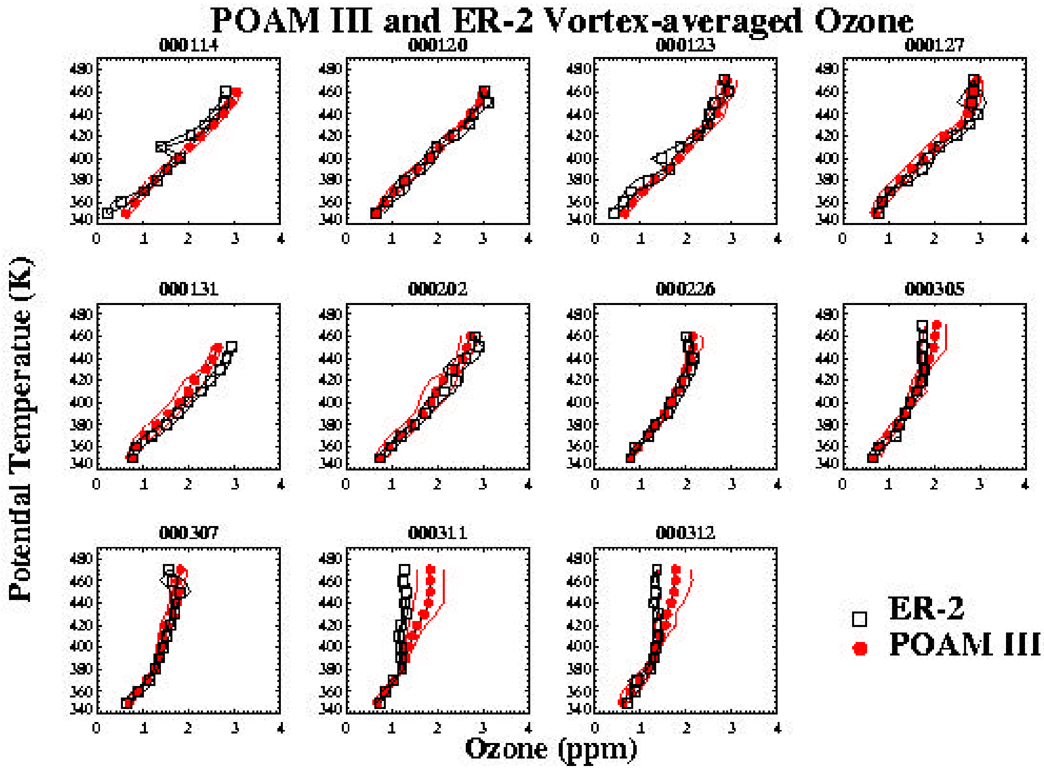
POAM III and ER-2 Vortex-averaged Ozone
000114
000120
000123
000127
000131
000202
000226
000305
000307
000311
000312
Potential Temperatue (K)
Ozone (ppm)
ER-2
POAM III

Figure 6

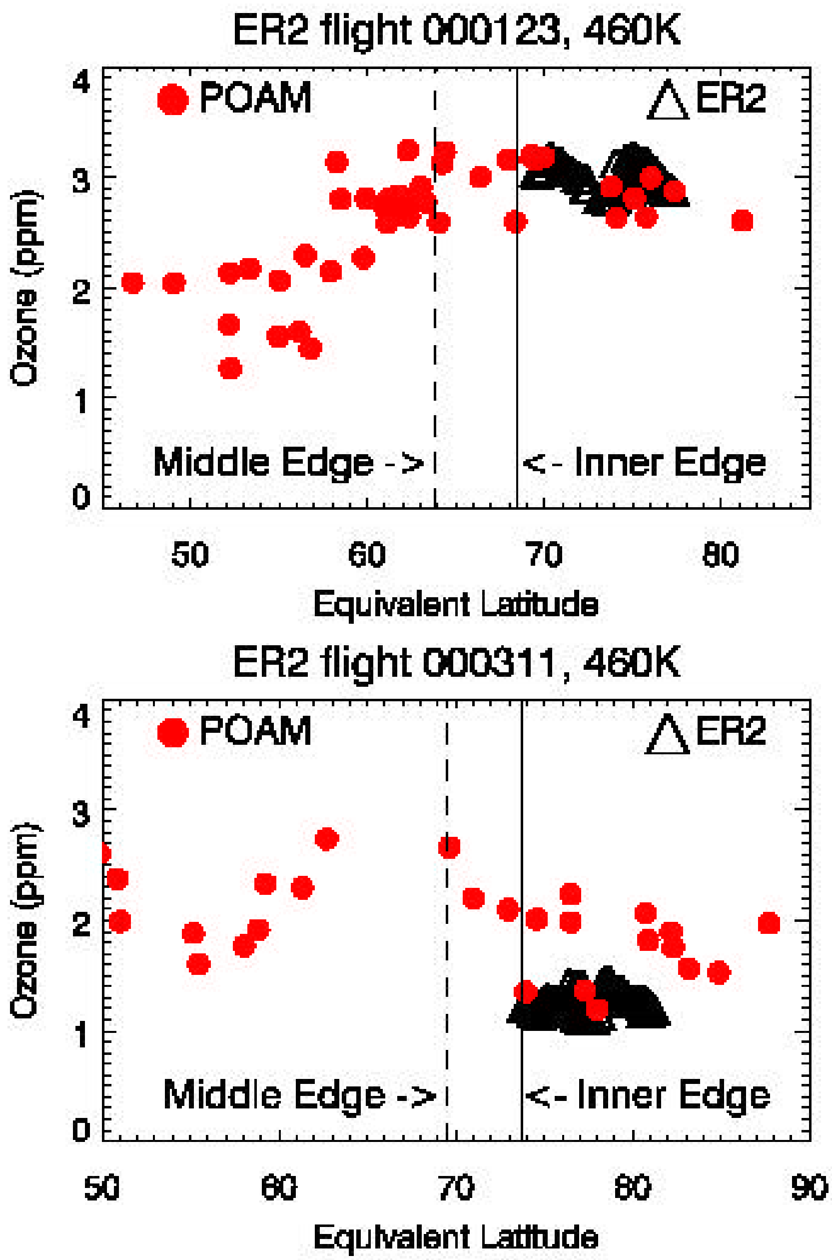
ER2 flight 000123, 460K
POAM
ER2
Middle Edge ->
<- Inner Edge
Ozone (ppm)
Equivalent Latitude
0
1
2
3
4
50
60
70
80
ER2 flight 000311, 460K
POAM
ER2
Middle Edge ->
<- Inner Edge
Ozone (ppm)
Equivalent Latitude
0
1
2
3
4
50
60
70
80
90

Figure 7

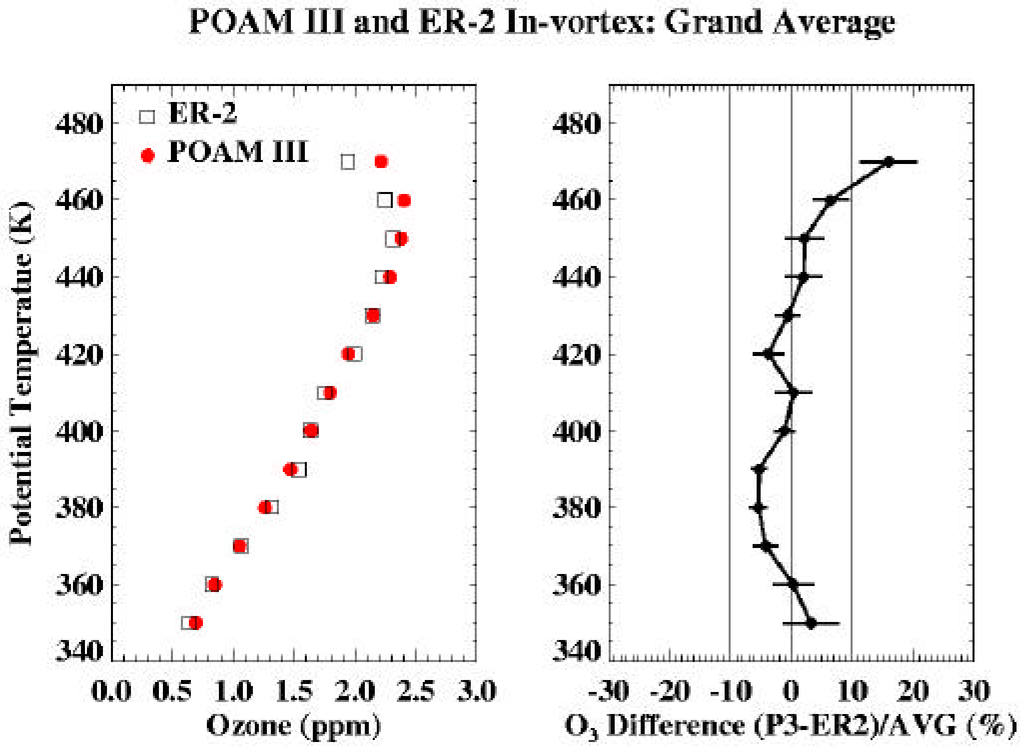
POAM III and ER-2 In-vortex: Grand Average
ER-2
POAM III
Potential Temperatue (K)
480
460
440
420
400
380
360
340
0.0 0.5 1.0 1.5 2.0 2.5 3.0
Ozone (ppm)
-30 -20 -10 0 10 20 30
O3 Difference (P3-ER2)/AVG (%)

Figure 8

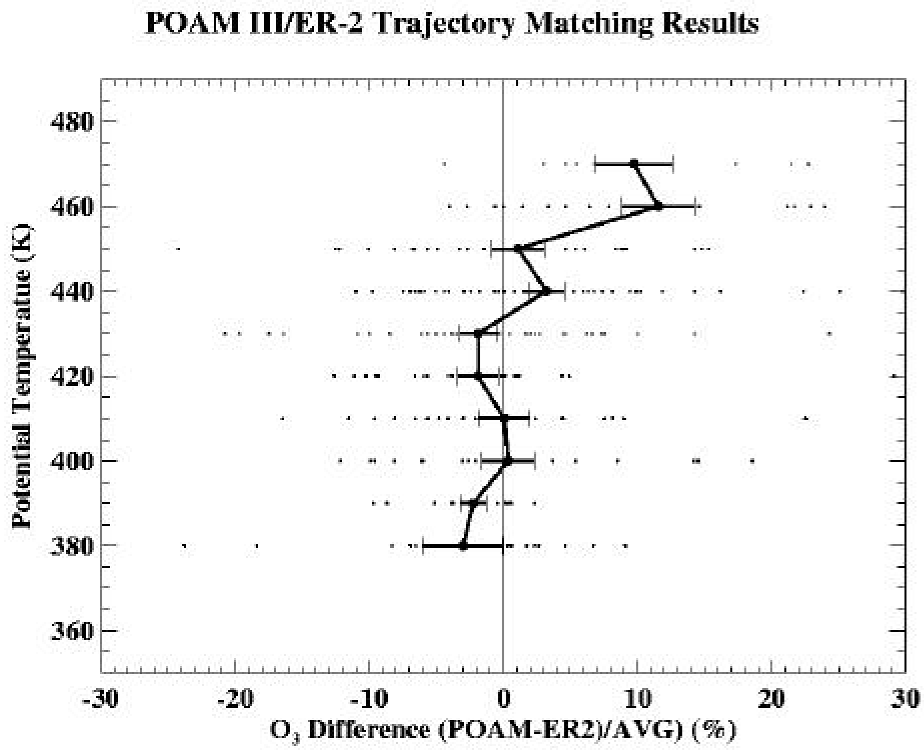
POAM III/ER-2 Trajectory Matching Results
480
460
440
420
400
380
360
Potential Temperatue (K)
-30
-20
-10
0
10
20
30
O3 Difference (POAM-ER2)/AVG) (%)

Figure 9

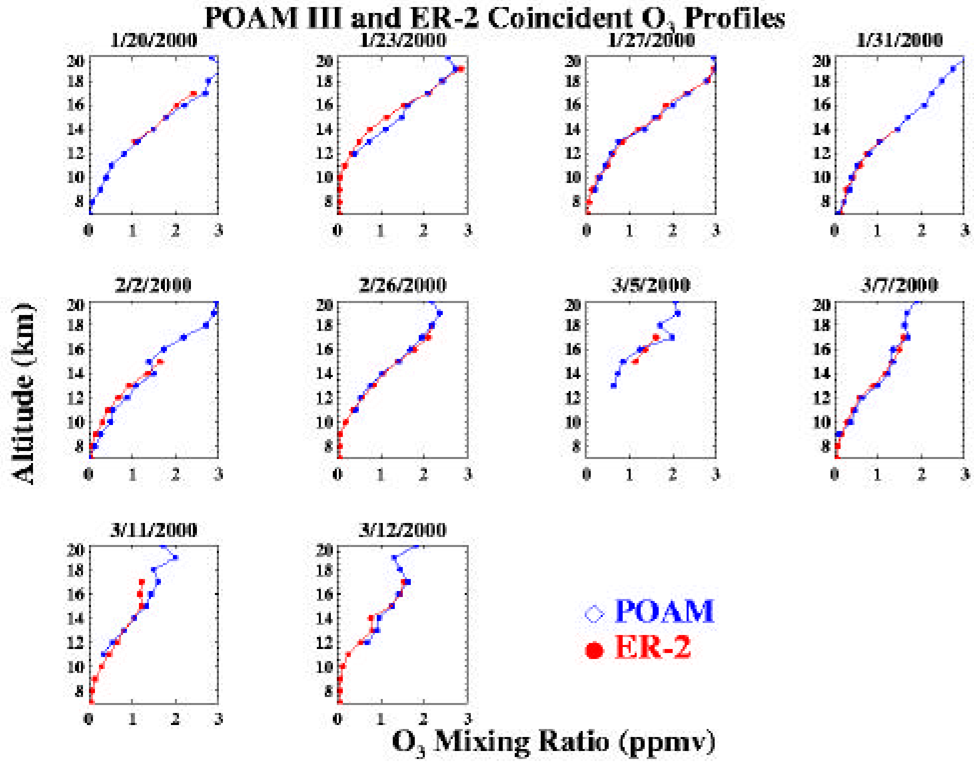

POAM III and ER-2 Coincident O_3 Profiles
1/20/2000
1/23/2000
1/27/2000
1/31/2000
2/2/2000
2/26/2000
3/5/2000
3/7/2000
3/11/2000
3/12/2000
Altitude (km)
O_3 Mixing Ratio (ppmv)
POAM
ER-2

Figure 10

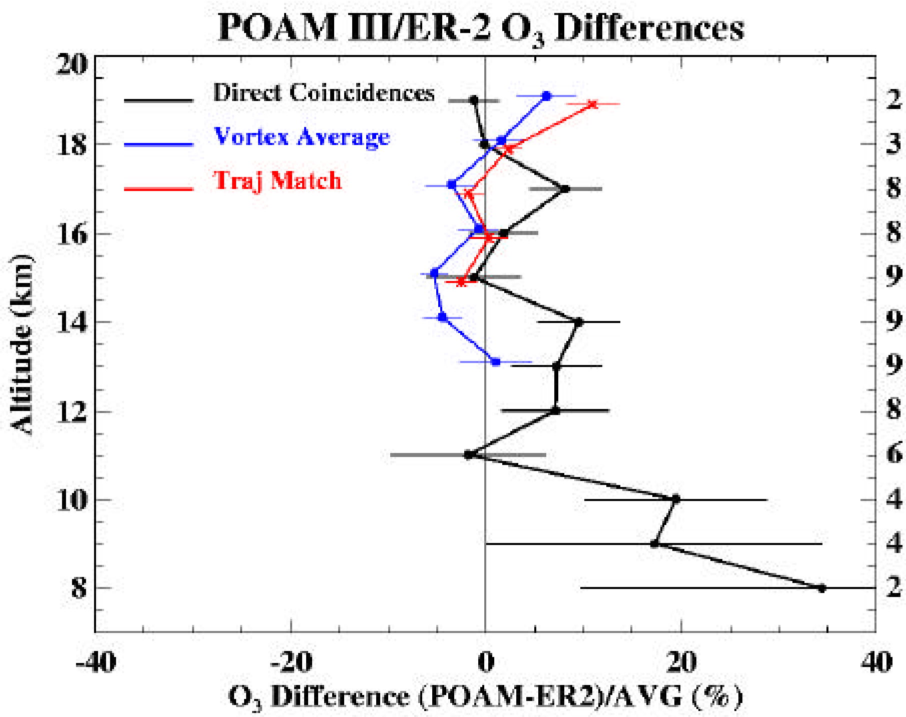
POAM III/ER-2 O_3 Differences
Direct Coincidences
Vortex Average
Traj Match
Altitude (km)
20
18
16
14
12
10
8
2
3
8
8
9
9
9
8
6
4
4
2
-40
-20
0
20
40
O_3 Difference (POAM-ER2)/AVG (%)

Figure 11

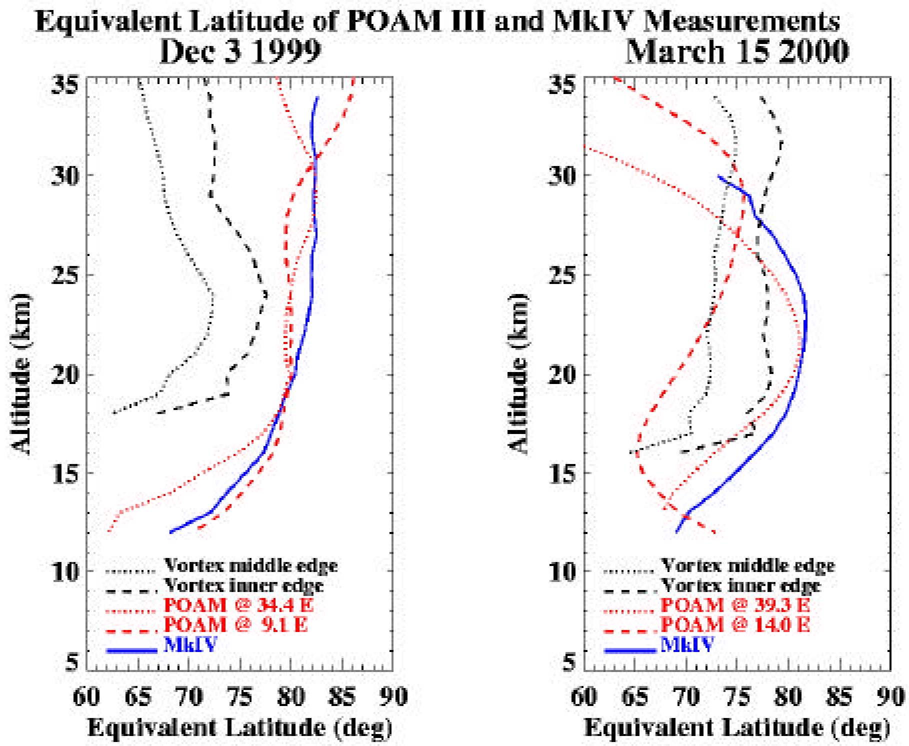
Equivalent Latitude of POAM III and MkIV Measurements
Dec 3 1999
March 15 2000
Altitude (km)
Equivalent Latitude (deg)
Vortex middle edge
Vortex inner edge
POAM @ 34.4 E
POAM @ 9.1 E
MkIV
POAM @ 39.3 E
POAM @ 14.0 E
35
30
25
20
15
10
5
60
65
70
75
80
85
90

Figure 12

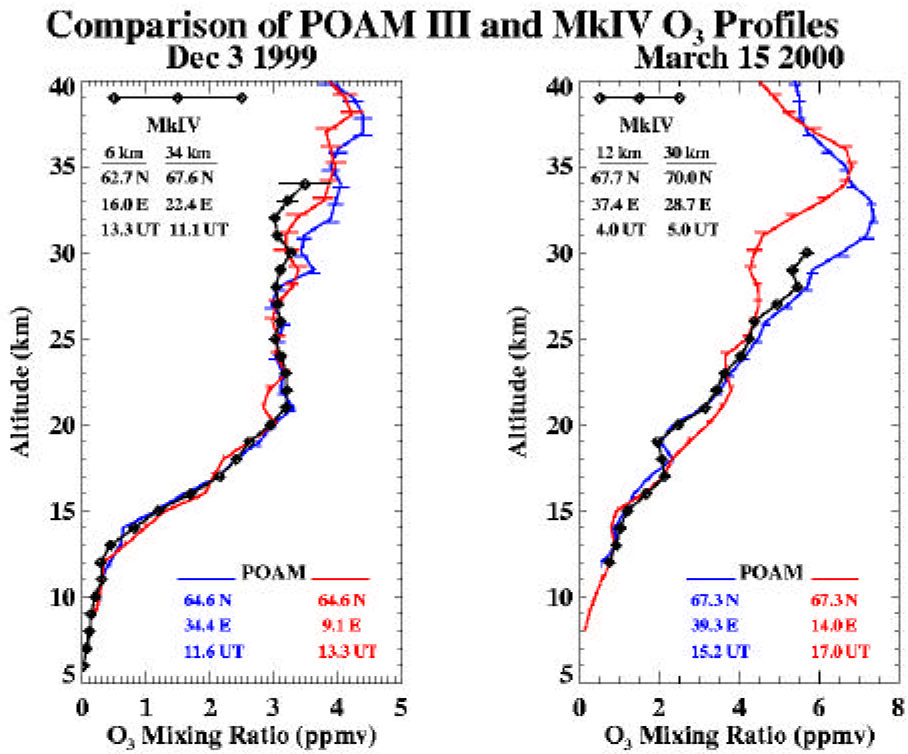
Comparison of POAM III and MkIV O3 Profiles
Dec 3 1999
March 15 2000
MkIV
6 km 34 km
62.7 N 67.6 N
16.0 E 22.4 E
13.3 UT 11.1 UT
12 km 30 km
67.7 N 70.0 N
37.4 E 28.7 E
4.0 UT 5.0 UT
POAM
64.6 N 64.6 N
34.4 E 9.1 E
11.6 UT 13.3 UT
67.3 N 67.3 N
39.3 E 14.0 E
15.2 UT 17.0 UT
Altitude (km)
O3 Mixing Ratio (ppmv)

<u>Figure 13</u>

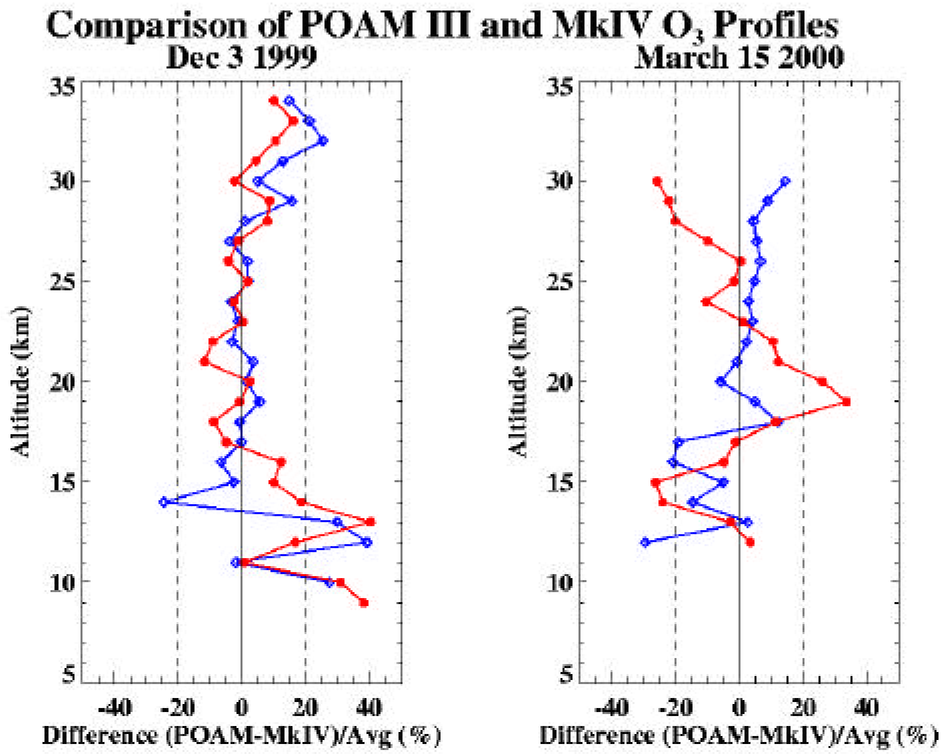

Comparison of POAM III and MkIV O3 Profiles
Dec 3 1999
March 15 2000
Altitude (km)
35
30
25
20
15
10
5
-40
-20
0
20
40
Difference (POAM-MkIV)/Avg (%)

Figure 14

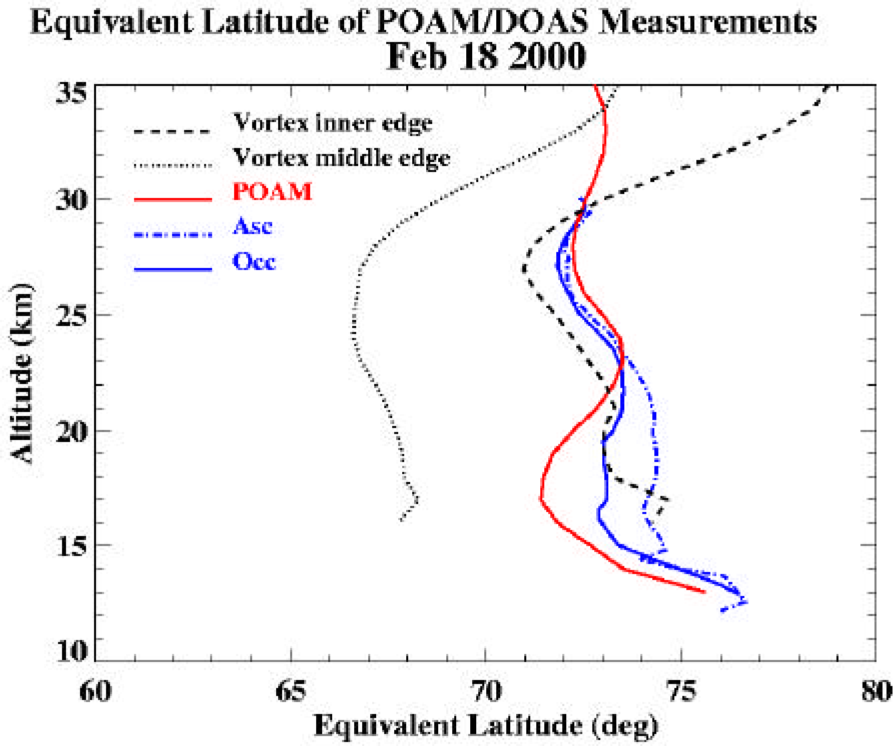
Equivalent Latitude of POAM/DOAS Measurements
Feb 18 2000
Vortex inner edge
Vortex middle edge
POAM
Asc
Occ
Altitude (km)
Equivalent Latitude (deg)
35
30
25
20
15
10
60
65
70
75
80

Figure 15

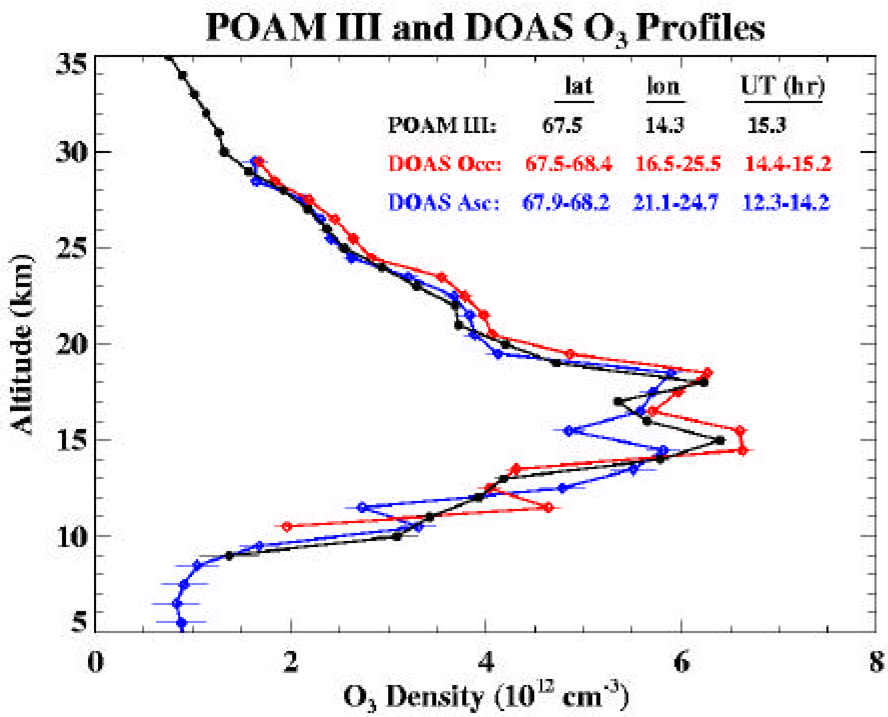

POAM III and DOAS O3 Profiles
lat
lon
UT (hr)
POAM III: 67.5 14.3 15.3
DOAS Occ: 67.5-68.4 16.5-25.5 14.4-15.2
DOAS Asc: 67.9-68.2 21.1-24.7 12.3-14.2
Altitude (km)
35
30
25
20
15
10
5
0
2
4
6
8
O3 Density (10^12 cm^-3)

Figure 16

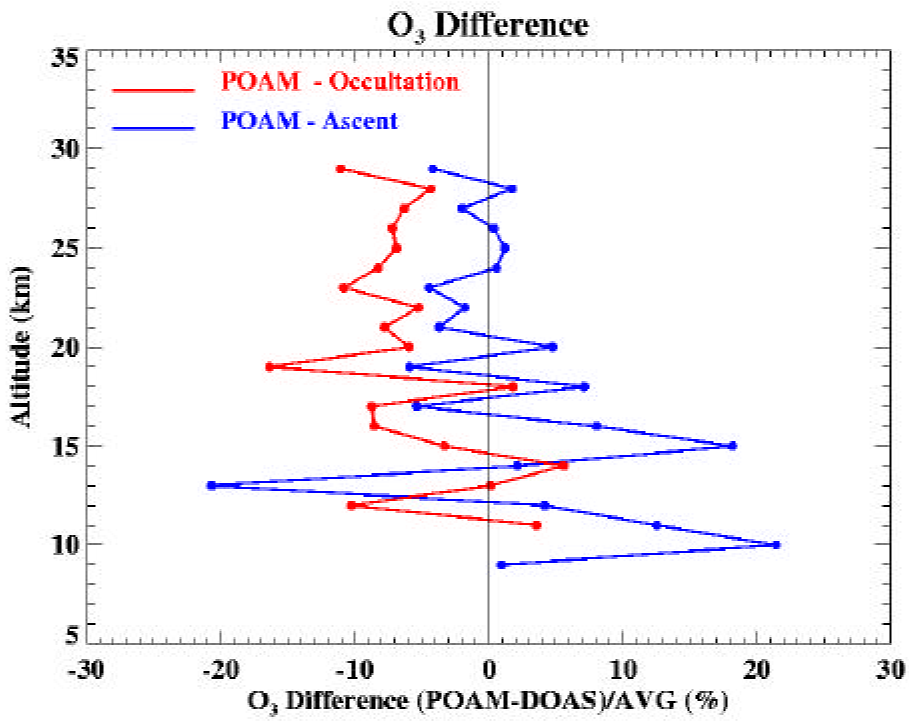

O_3 Difference
POAM - Occultation
POAM - Ascent
Altitude (km)
35
30
25
20
15
10
5
-30
-20
-10
0
10
20
30
O_3 Difference (POAM-DOAS)/AVG (%)

Figure 17

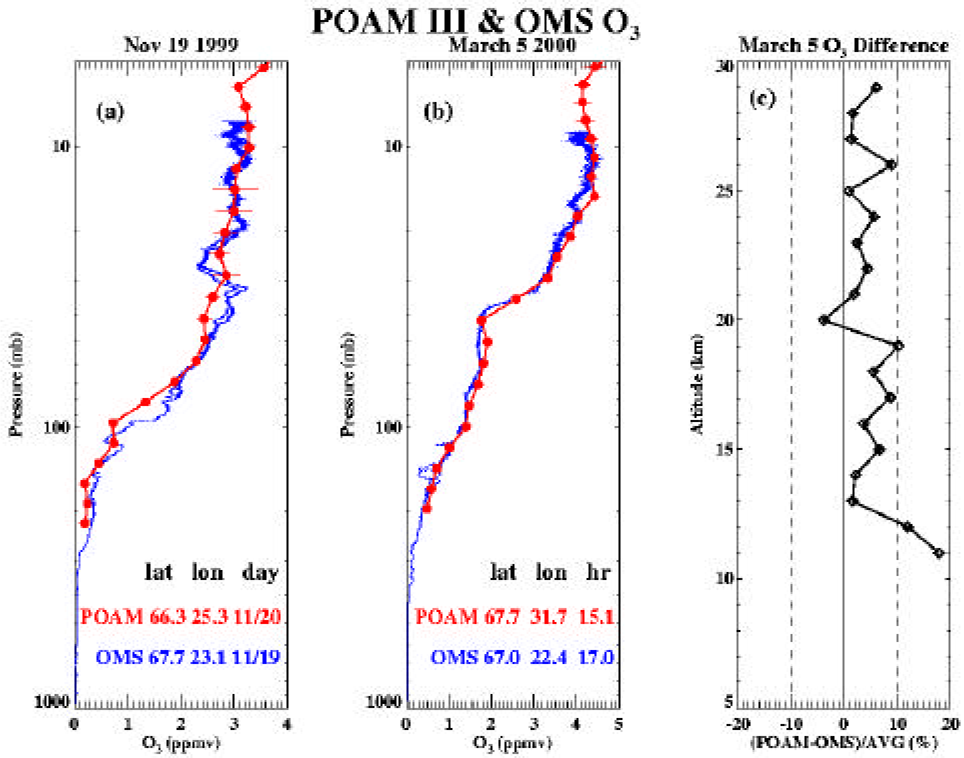

POAM III & OMS O_3
Nov 19 1999
March 5 2000
March 5 O_3 Difference
(a)
(b)
(c)
Pressure (mb)
Altitude (km)
O_3 (ppmv)
(POAM-OMS)/AVG (%)
lat lon day
POAM 66.3 25.3 11/20
OMS 67.7 23.1 11/19
lat lon hr
POAM 67.7 31.7 15.1
OMS 67.0 22.4 17.0

Figure 18

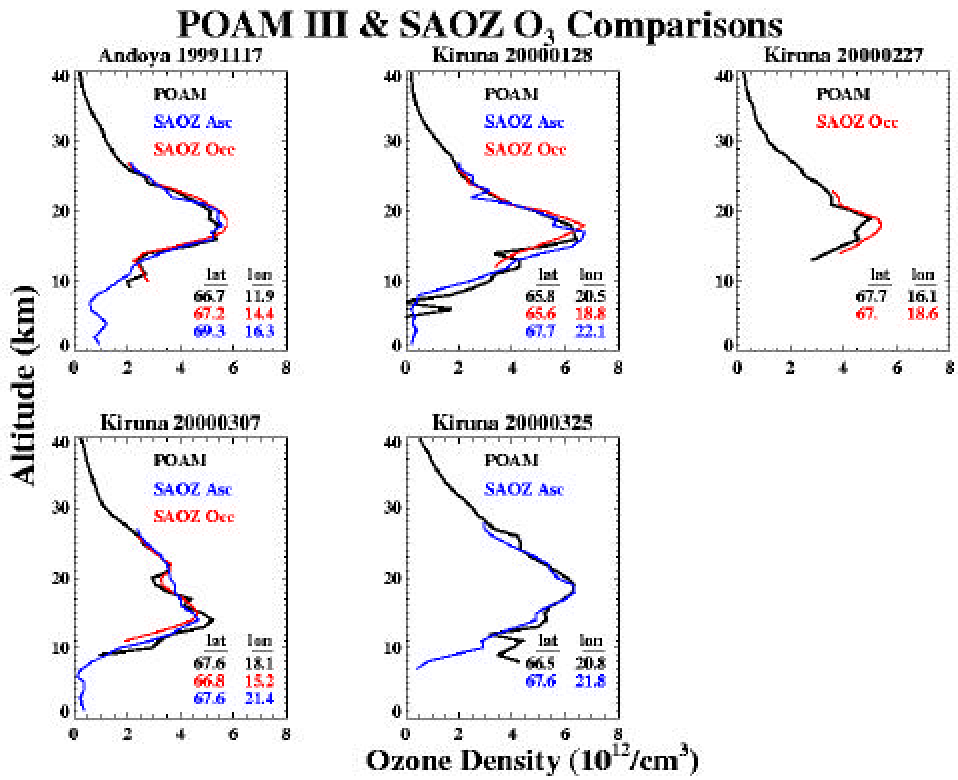
POAM III & SAOZ O_3 Comparisons
Andoya 19991117
Kiruna 20000128
Kiruna 20000227
Kiruna 20000307
Kiruna 20000325
POAM
SAOZ Asc
SAOZ Occ
lat lon
66.7 11.9
67.2 14.4
69.3 16.3
65.8 20.5
65.6 18.8
67.7 22.1
67.7 16.1
67. 18.6
67.6 18.1
66.8 15.2
67.6 21.4
66.5 20.8
67.6 21.8
Altitude (km)
Ozone Density (10^{12}/cm^3)

Figure 19

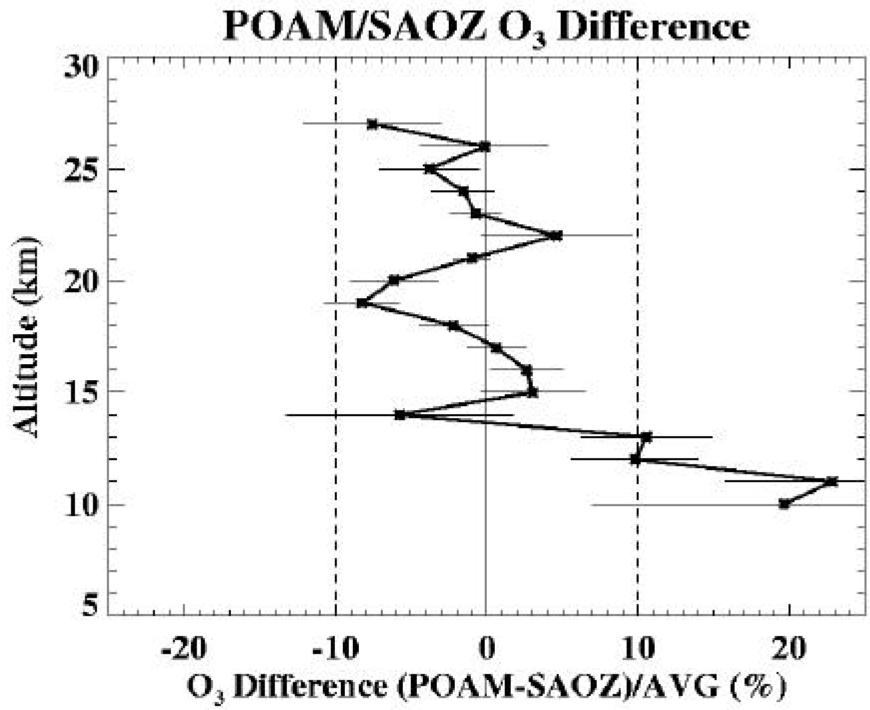
POAM/SAOZ O3 Difference
Altitude (km)
30
25
20
15
10
5
-20
-10
0
10
20
O3 Difference (POAM-SAOZ)/AVG (%)

Figure 20

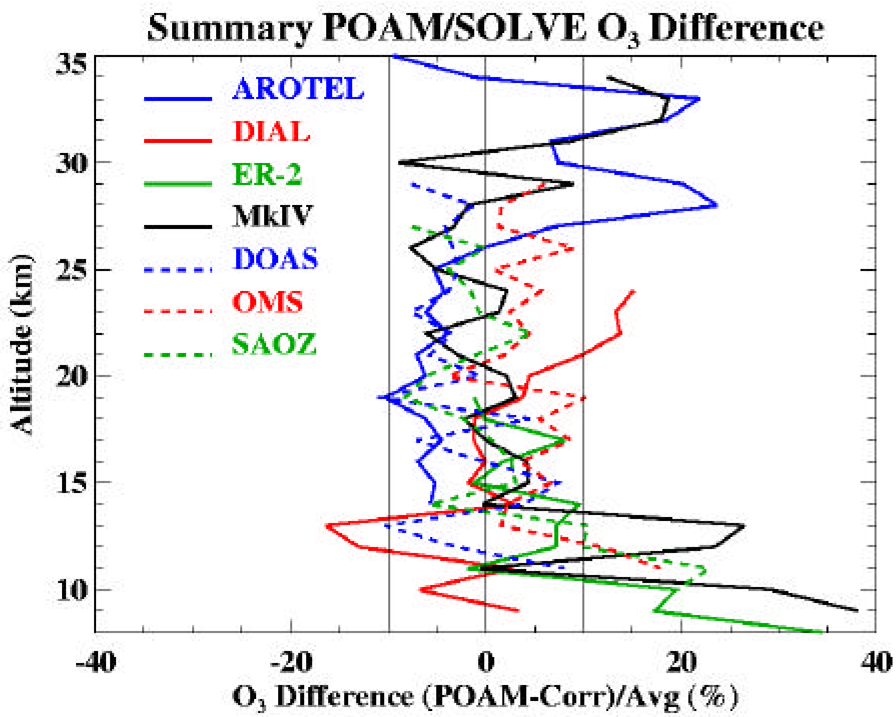

Summary POAM/SOLVE O_3 Difference
AROTEL
DIAL
ER-2
MkIV
DOAS
OMS
SAOZ
Altitude (km)
35
30
25
20
15
10
-40
-20
0
20
40
O_3 Difference (POAM-Corr)/Avg (%)

Figure 21